2019

Geothermal Resource Assessment of Mississippi

Adam Blake Goodwin
University of Mississippi

GEOTHERMAL RESOURCE ASSESSMENT OF MISSISSIPPI

A Thesis
Presented in partial fulfillment of the requirements
for the degree of Master of Science
in the Department of Geology and Geological Engineering
The University of Mississippi

by

ADAM B. GOODWIN

May 2019

ABSTRACT

Geothermal energy is exploited through the process of using hot water or steam extracted from reservoirs of geothermal heat in Earth's crust which is derived from the upward convection and conduction of heat from Earth's mantle and core. This energy can be harnessed to power geothermal heat pumps, heat water, or to generate electricity. Previous geothermal assessments of Mississippi have been locally focused, either in the southern Mississippi River flood plains or in eastern north central Mississippi at an active lignite coal mine. The focus of this project was to calculate and map heat flow estimates within the entire state of Mississippi. Assessment of well log datasets, estimating thermal conductivity values within broad stratigraphic intervals, and creating a new geothermal gradient model allowed me to delineate patterns of temperature resources sufficient for future geothermal applications. This study also provides preliminary geophysical evidence of a high geothermal temperature gradient spatially associated with major tectonic features in Mississippi. The potential economic reward for mapping this clean, renewable energy source could be enormous. The overall environmental impacts are considerably lower than fossil fuel and nuclear power plants. The future of geothermal systems also has the potential for lower impacts in comparison to other renewables like solar, biomass, and wind. This is because the power source is contained underground, and the energy conversion equipment is relatively compact making the overall environmental footprint very small in comparison with other sources.

DEDICATION

This thesis is dedicated to Grace and Meghan Goodwin, I would not have been able to complete this without the love, patients, and encouragement from both of you.

LIST OF ABBREVIATIONS AND SYMBOLS

BHT	Bottom hole temperature
DEM	Digital elevation model
EGS	Enhanced geothermal systems
IDW	Inverse distance weighting
ISO	Isopach
TC	Thermal conductivity
Th	Thorium
K	Potassium
U	Uranium
Cz	Cenozoic
K-Pg	Cretaceous – Paleogene
LK	Lower Cretaceous
Pz	Paleozoic
UK	Upper Cretaceous
UJ	Upper Jurassic
°C/km	Degrees Celsius per kilometer
Δ °C	Change in temperature, degrees Celsius
kwh	Kilowatt hour
MW	Megawatts
mW/m^2	Milliwatts per square meter
W/m^2	Watts per square meter
W/m·K	Watts per meter degrees kelvin
WTC	Weighted thermal conductivity
AAPG	American Association of Professional Geologist
DOE	Department of Energy

GSNA	Geothermal Survey of North America
MDEQ	Mississippi Department of Environmental Quality
MISB	Mississippi Interior Salt Basin
OPEC	Organization of the Petroleum Exporting Countries
SMU	Southern Methodist University
USEIA	United States Energy Information Agency

ACKNOWLEDGMENTS

I would first like to thank the Department of Geology and Geological Engineering along with my thesis committee, which consisted of Dr. Louis Zachos, Dr. Greg Easson, and Dr. Lance Yarbrough. I met with Dr. Zachos during my first semester with an idea on doing a project that something to do with geothermal resources. Throughout my thesis, Dr. Zachos's experience in ArcGIS, geology, and engineering applications guided me through this project. Dr. Zachos is a patient mentor, great advisor, and most of all a good friend, thank you for all your help in our weekly meetings.

I am very grateful for Mississippi Mineral Resource Institute for providing a sponsorship for my studies during my final year at the University of Mississippi. Dr. Easson surprised me with the opportunity to continue my research with a research assistantship position, and I want to say thank you very much. Without it I doubt I would have had time to finish with my busy family life. I would also like to thank Dr. Yarbrough for his support with the engineering calculations he helped derive. The complex raster creation and processing I was preforming would sometimes cloud my judgement and he was always there to assist with equations. Thank you all very much, I will never forget all the help you have given me. Thank you to Dr. David Dockery, Mississippi Department of Environmental Quality, for sending me the available data set for the state of Mississippi and for your geological interpretations.

I would also like to thank Dr. Murlene Clark for the motivation, help, and encouragement to go for my masters. Without your help I would have never submitted my application for the geological program. Her personality and intelligence have provided so much inspiration and I want to thank you for everything you have done for me. I also want to thank Dr. David Allison for all the opportunities he has given me preforming undergraduate research along with the mentorship he provided in making me a better geologist.

Lastly, I want to thank my parents Peggy R. Goodwin, Gary Goodwin, my brother and Zach Goodwin and wife Jennifer Goodwin, and my grandparents Libby Williford and Henry Williford. I am sincerely thankful for all the love, support, and encouragement you all have given me. Without it I would not be where I am today, thank you so much.

TABLE OF CONTENTS

LIST OF TABLES

LIST OF FIGURES

CHAPTER 1

INTRODUCTION

In the fall of 1973 when the Organization of the Petroleum Exporting Countries (OPEC) imposed a boycott on the exportation of oil to the United States, there was a focusing of attention in the United States to find and develop alternate energy sources (Luper and Report, 1978). This focus continues today even as fossil fuels continue to be available and renewable energy pushes forward as green-technology advances. Geothermal resources are baseload, generating constant power. Enhanced geothermal systems (EGS), described below, offer the opportunity to access this enormous domestic clean energy source while emitting little to no greenhouse gases (Geothermal Technologies Office, 2006).

Enhanced geothermal systems are man-made, closed-cycle systems, created where there is hot rock but with little or no natural permeability or fluid saturation (Geothermal Technologies Office, 2006). Since EGS's only prerequisite is heat, it can be deployed nearly anywhere there is rock hot enough to produce power. There are different types of geothermal power plants, but for places where the water temperature is around 150°C - 200°C a binary plant is used (Richards, 2008). In a non-closed loop system heat and electricity produced by EGS harness the energy from hot rock by fracturing the target zone, circulating water through the system, to the surface where the water heats a working fluid such as isopentane, which boils at a lower temperature for vapor production. This gas is used to drive the turbines and create electricity. The isopentane then condenses back to its liquid state and is reused. The water is re-injected into the rock, where the process begins again.

The most common type of geothermal power plant in operation today is the flash steam power plant. These plants operate where fluid temperatures are around 100°C - 150°C. The fluid is pumped under high pressure into a tank at the surface and held at much lower pressure, causing some of the fluid to vaporize. The vapor is then used to drive a turbine to create electricity, while the remaining fluid can be flashed again in a second tank to utilize even more energy.

In a closed loop system heat pumps circulate an anti-freeze solution through a closed loop usually made of plastic tubing that is buried in the ground or submerged in water. A heat exchanger transfers heat between the refrigerant in the heat pump and the antifreeze solution in the closed loop system. One variation of this system is called direct exchange and does not use a heat exchanger. Instead it pumps the refrigerant through copper tubing that is buried in the ground and circulates refrigerant through the ground to directly heat or cool homes and buildings.

The United States Energy Information Administration (EIA) estimates that an average American household uses 12,000-kilowatt hour (kWh) of electricity per year (USEIA, 2012). In 2011, Southern Methodist University researchers estimated that Mississippi's geothermal technical potential at a 14% recovery was approximately 60,000 megawatts (MW). This is enough power to supply electricity to more than sixty million homes (Lindsey, 2012). In a survey conducted by the United States Census Bureau, Mississippi has an estimated 1.3 million homes (Lindsey, 2012). EGS could potentially make Mississippi an energy exporter throughout the south.

The primary purpose of this study was to calculate and map heat flow within the state of Mississippi (FIG. 1) in order to delineate areas of temperature resources sufficient for geothermal

applications. A new evaluation of the thermal gradient was performed in order to update the heat flow calculations and access the true geothermal potential. This assessment of the geotemperature regime is the first step in the exploitation process and will serve to emphasize more prospective areas in MS for future development. The use of the new heat flow maps will help academic, governmental, and civilian researchers consider the use of geothermal as a potential energy resource for the state of Mississippi. Mississippi is an ideal area for geothermal evaluation because there has been significant hydrocarbon exploration providing an abundance of well data for the temperature assessment

Figure 1 — Mississippi and the Mississippi Interior Salt Basin.

CHAPTER 2

GEOLOGICAL SETTING

Gulf of Mexico Structural Setting

The Gulf of Mexico is a divergent margin basin created by extensional rift tectonics and wrench faulting (Miller, 1982; Pilger, 1981; Salvador, 1987; Winker and Buffler, 1988). The formation of the Gulf of Mexico included a phase of crustal extension and thinning, a phase of rifting and sea floor spreading, and a phase of thermal subsidence (Nunn, 1984). The structural and stratigraphic framework of the region, including the Mississippi Interior Salt Basin (MISB), was established during the Triassic and Jurassic (FIG. 2) (Salvador, 1987).

Figure 2 — Map illustrating opening of the Gulf of Mexico by movement of the Yucatan Block and Florida-Bahama blocks of continental/transitional crust (modified from Redfern, 2001; Hine, 2013).

Based on the dispersal of crust type, Sawyer et al. (1991) proposed the following model for the evolution of the Gulf of Mexico and relationship to the MISB. The Late Triassic-Early Jurassic early rifting phase was characterized by the formation of large and small half grabens bounded by listric normal faults. The half grabens were filled with non-marine siliciclastic sediments (red-beds) and volcaniclastic sediments. The Middle Jurassic phase of rifting, crustal weakening, and the formation of transitional crust was characterized by the evolution of alternating basement highs and lows and the accumulation of thick salt deposits in the lows, collectively known as the Louann Formation.

The Late Jurassic phase of sea floor spreading and oceanic crust formation in the deep Central Gulf of Mexico was characterized by a regional marine transgression resulting from crustal cooling and subsidence. Subsidence continued into the Early Cretaceous, and a carbonate shelf margin developed along the tectonic hinge zone marked by differential subsidence between thick and thin transitional crust. During the Early Cretaceous, erosional events occurred in the Valanginian, in the Aptian, in the Lower Albian, and in the Upper Albian reflecting times of sea-level fall in the Gulf (Yurewicz et al., 1993). During the Late Cretaceous (mid-Cenomanian), this pattern of deposition was interrupted by a period of igneous activity (including forming the Jackson Dome) and global sea-level fall (Salvador, 1991).

This major lowering of sea level resulted in the exposure of a shallow Cretaceous platform margin that rimmed the Gulf of Mexico. Mesozoic and Cenozoic strata in this region were deposited as part of a seaward-dipping wedge of sediment that accumulated in differentially subsiding basins on the passive margin of the North American continent (Martin, 1978). Basement cooling and subsidence resulted in the filling of accommodation space throughout the Jurassic. Structural elements that have affected orientation of these strata include basement features associated with plate movement and features formed due to halokinesis or movement of the

Jurassic salt. The tectonic processes responsible for the formation of the Gulf of Mexico and the peripheral sedimentary basins produced a significant thickness of sedimentary rocks suitable for hydrocarbon traps.

Mississippi's Geological Setting

The burial and thermal history of the Mississippi Interior Salt Basin are directly correlated with the tectonic and depositional history of the basin, which are in turn closely related to the origin of the Gulf of Mexico (Wood and Walper, 1974). The distribution of sediment was significantly impacted by the paleotopography of the region, where positive areas within basins and along basin margins provided sources for Mesozoic terrigenous sediments (FIG. 3) (Mancini et al., 1985b).

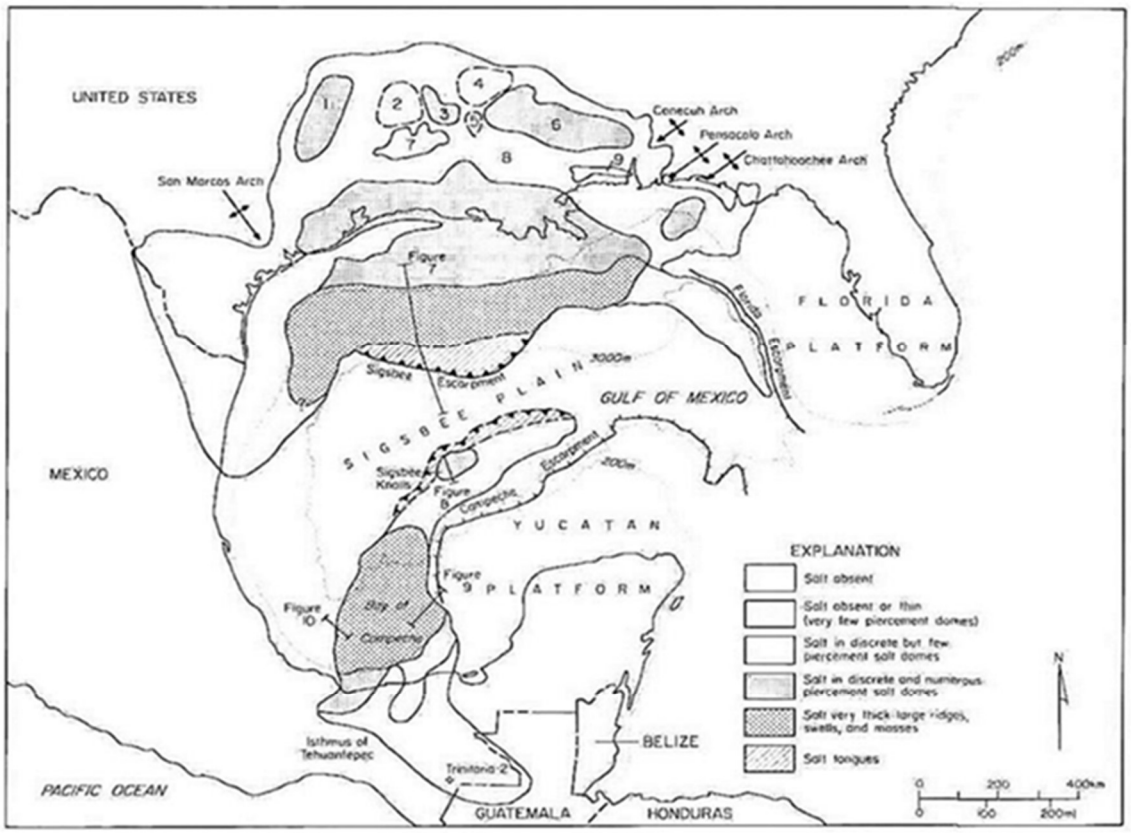

Figure 3 — Distribution of salt deposits. 1: East Texas Basin, 2: Sabine Uplift, 3: North Louisiana Salt Basin, 4: Monroe Uplift, 5: La Salle Arch, 6: Mississippi Interior Salt Basin, 7: Jasper arch, 8: Adams County High, 9: Wiggins Uplift. (Salvador, 1987).

The Mississippi Interior Salt Basin is a major negative structural feature in the northeastern Gulf of Mexico and is classified as the interior fracture portion of a margin sag basin (Kingston et al., 1983). This extensional basin was an actively subsiding depository throughout the Mesozoic and Cenozoic. Wilson (1975), interpreted the Mississippi Interior Salt Basin to be an area of thinned granitic continental crust, based on gravity data. Crustal thinning resulted from tectonic extension within the region occurred during the rifting of the Gulf of Mexico in the early Mesozoic. This thinning of crust established a subsiding basin cratonward of the rifted and elevated continental margin (Wood and Walper, 1974).

Halokinesis of the Jurassic Louann Salt has produced a diverse set of structural features throughout the northeastern Gulf of Mexico (Martin, 1978). The salt related structures include diapirs, anticlines, extensional fault and half graben systems. Regional structural features resulting from salt movement includes; the regional peripheral fault trend, the Mobile graben, numerous salt domes and anticlines. This halokinetically-related structural deformation forms petroleum traps in the region (FIG. 4).

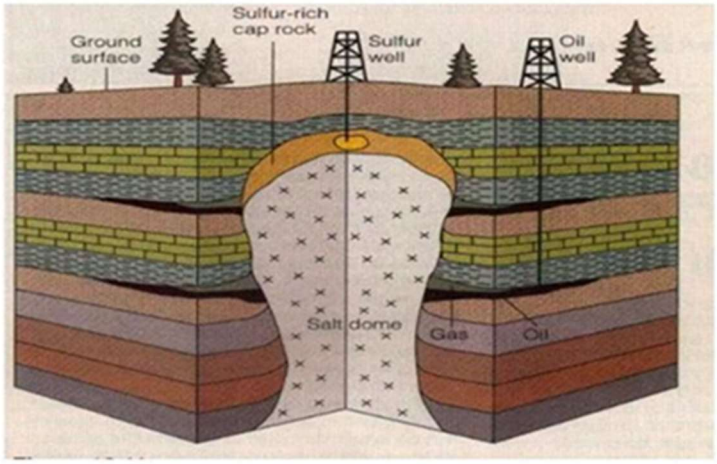

Figure 4 — A typical salt dome (Setterfield, 2015).

Mississippi's Interior Salt Basin

Within the Gulf Coastal area there are five distinct regions which are known as salt basins. These basins were centers of thick accumulations of sedimentary salt with density differences between the salt and the sediment created by later deposition that caused the salt to flow. Salt structures known as diapirs are a direct result of overburden pressures (FIG.5). One of these basins is the Mississippi Interior Salt Basin which extends in a southeastern direction from northeast Louisiana across Mississippi to southwestern Alabama.

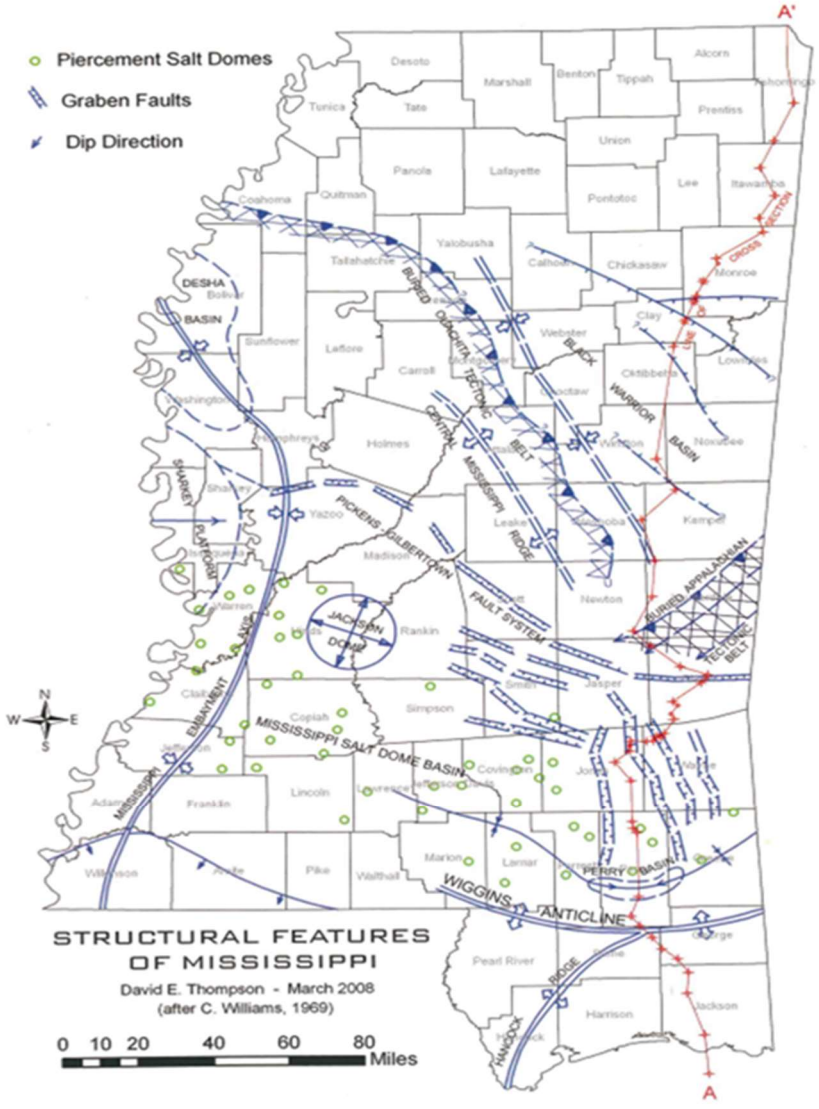

Figure 5 — Structural features of Mississippi (Dockery, 2016).

This basin is about 250 miles long, averages about 60 miles wide and contains 148 known salt domes (Beckman J.D. et al., 1990). The depth to salt in the domes ranges from 400 feet to more than 15,000 feet (Anderson et al., 1973). The tops of 44 of the domes lie between 2,000 and 4,000 feet deep, while the tops of only two salt domes are less than 1,000 feet deep and the tops of 12 salt domes are more than 10,000 feet deep. The areal distribution of depths to salt is irregular, however the deeper domes occur in the northern part of the basin and the shallower domes occur in the southern section. The MISB lies within parts of two physiographic regions: The Mississippi River Alluvial Plain in the northwest, and the Gulf Coastal Plain in the southeast. The Gulf Coastal Plain is characterized by pine-forested hilly uplands traversed by alluviated stream valleys while the Mississippi River Alluvial Plain is a southward sloping plain with little relief.

Salt Domes as a Possible Source of Geothermal Energy

The Mississippi Interior Salt Basin is one of the most oil and gas productive basins in the on-shore Gulf Coastal Plain and is an important province in North America for oil and gas deposits. The economic importance of this salt basin's oil and gas accumulations pales in comparison to the potential value of its thermal energy. This basin has produced nearly 2 billion barrels of oil and over 6 trillion cubic feet of natural gas. It is the largest basin in the southeast while also having the greatest potential for identifying underdeveloped plays and reservoirs (Mancini et al., 2001).

The salt within the MISB has potential economic importance that has often been overlooked (FIG. 6). It has one of the highest thermal conductivities of all minerals (Jacoby and Paul, 2003). Also, its favorable heat capacity fluctuates significantly with temperature change. At high temperatures and pressure, salt becomes plastic, which has become widely accepted as the reason for the formation of domal structures. These domes/diapers are characteristic of geopressurized zones resulting from the fact that to create many of these subsurface features it requires a massive amount of localized heat conducted by salt.

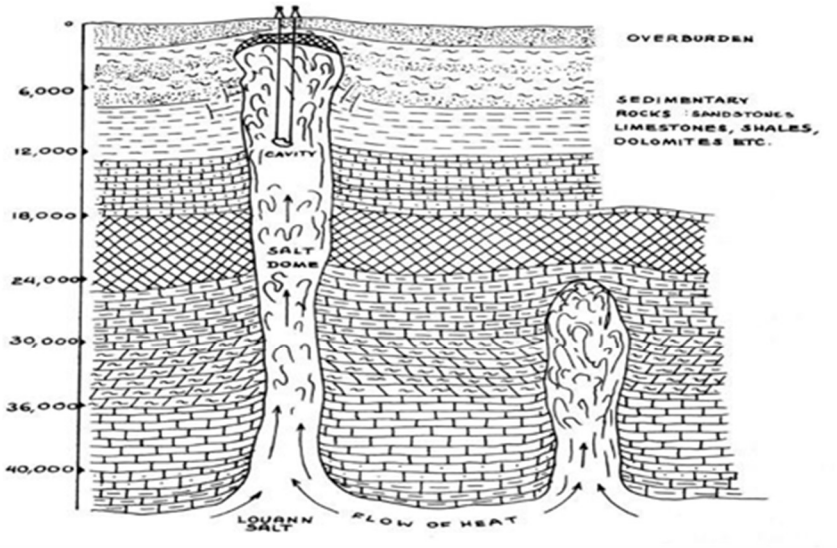

Figure 6 — Typical section trough a Gulf region salt dome and its surrounding strata. Since the salt has a greater thermal conductivity than the surrounding rock, it generates a thermal anomaly (Jacoby and Paul, 2003).

Because of the deep-seated origin and inherent high thermal conductivity of salt bodies, surrounded by formations with low thermal conductivity, salt domes represent a superlative medium for geothermal heat conduction, collection, and utilization. Temperature logs in various locations have proven that temperatures of the order of 330 °F at 10,000 ft., 455 °F at 15,000 ft., and 580 °F at 20,000 ft. are representative of salt domes. This temperature gradient is about four times that of the normal geothermal gradient in crustal rocks.

Jackson Dome

The Jackson Dome is located in the northeastern portion of Hinds County and adjoining Rankin and Madison Counties (FIG. 7). The Jackson Dome is a broad structural uplift, roughly circular, around 25 mi in diameter, and is formed by the arching of strata over a deep-seated igneous plug. The Jackson Dome is a result primarily of crustal warping, which accompanied the igneous activity, with secondary compaction of shales relative to sandstone and igneous rock (Monroe, 1954). The igneous activity in the Late Cretaceous was followed by the deposition of reefal carbonates, termed the Jackson Gas Rock, that formed in association with the uplift (Ewing, 1991). The Jackson Dome is an excellent example of a structural-stratigraphic trap (FIG. 8) for hydrocarbons and has been the site of significant natural gas and minor crude oil production since the 1930's (Saunders and Harrelson, 1992).

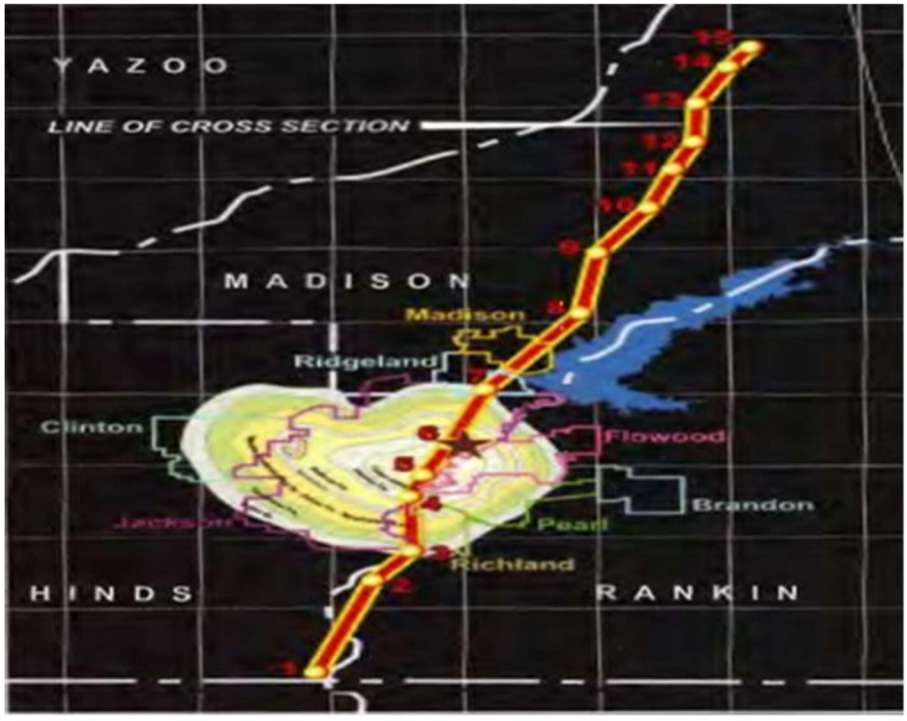

Figure 7 — Location and extent of Jackson Dome, with line of cross section for FIG. 8 (Dockery, 2016).

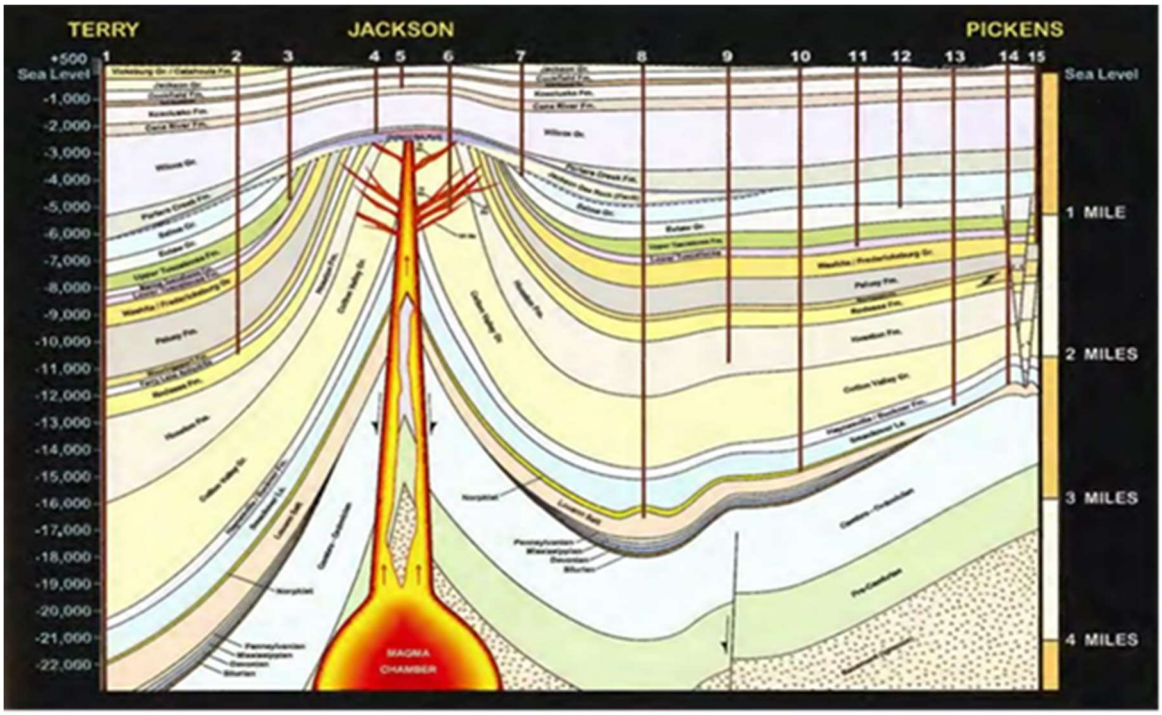

Figure 8 — South to north cross section of the Jackson Dome and Jackson Volcano (Dockery, 2016).

Igneous rocks analyzed from more than 200 samples, from 7 wells at the center of the dome, show different geochronological results ranging from 79 to 69 (± 2.9) Myr (Saunders and Harrelson, 1992). This is the youngest reported age of alkali igneous rocks in the northern Gulf Coast subsurface. This indicates that basement rifting, and volcanic/plutonic activity continued to at least nearly the end of the Cretaceous in the MSIB. This has important implication for Mesozoic sedimentation rates within the MISB and may have resulted in the relatively high geothermal gradient along the northern basin margin.

Many of the intrusions have undergone some form of hydrothermal alteration, but data generated by Saunders and Harrelson (1992) came from relatively unaltered to mildly altered samples of the Jackson Dome that appear to be representative of the overall igneous rock suite. These igneous rocks fall into two general types, phonolites and mafic-alkali rocks. The phonolite of the Jackson dome typically contains phenocrysts of sanidine and nepheline in a fine-grained groundmass of similar composition, while the mafic alkali rocks contain variable amounts of nepheline, and clinopyroxene (aegerine, aegeine-augite, or nephelinite, and jacupirangite based on their relative mineral abundances). Whole rock chemical analysis indicates that the rocks are nepheline-normative, silica deficient, with SiO_2 as low as 26.7 weight. percent, and are enriched in titanium TiO_2 as high as 8 percent, with Na + K commonly exceeding 14 percent. Heat from the earth is derived from two main sources: primordial heat left over from the formation of Earth and radioactive decay of the elements ^{232}Th, ^{235}U and ^{238}U, and ^{40}K. Heat generation within the igneous plug is likely to generate a geothermal heat source but this was not included for this study because of the depth and limited aerial extent of these plutons within the MISB.

One of the largest igneous structures in Mississippi, the Jackson Dome could potentially be a geothermal energy source, along with other buried plutons in the deep sediments of the Coastal Plains (Johns Hopkins University APL, 1978). This includes the Panther Burn Dome, Midnight Dome, Cary Dome, and just outside of Mississippi's border the EPP Dome. These buried plutons may be at temperatures elevated above the normal geothermal gradient as a result of heat generated from the decay of naturally occurring radioactive elements trapped by the insulating overlaying sedimentary deposits.

Heat Flow

Heat flow is the movement of heat (energy) from the interior of Earth to the surface. Heat escaping Earth's crust comes from two main sources; convection/conduction from the mantle (approximately 60%) and heat from radioactive elements in the crust, (^{232}Th, ^{235}U and ^{238}U, and ^{40}K; 40% all together (Pollack, 1982)). Heat flow is higher in areas with either high crustal radioactivity and/or where Earth's crust is thinner, such as mid-oceanic ridges or the Basin and Range Province of the western United States (Blackwell & Richards, 2011). High heat flow is also related to thermal plumes in the mantle which tend to thin the overlying crust. Heat flow is the driving force behind geothermal energy, and the reason that continuous power production can be achieved.

Heat flow is the product of thermal conductivity and temperature gradient. The standard units are milliWatt/meter^2 which translates into a flat plane 1 meter by 1 meter that indicates how much energy is transferred through the plane. For the heat flow value to be fully calibrated, the thermal conductivity and gradient must be measured or calculated. There are corrections that may be required based on average ground surface temperature and where the well was drilled. Examples of this issue are decreasing average ground surface temperature with increasing latitude, steep topography (north facing slopes of mountains are colder than south facing slopes), and geological structure (faults creating sharp changes in rock type with very different thermal conductivities).

Heat flow measurements within North America have recently been published as a map of the conterminous United States (Blackwell and Richards,2004), highlighting the thermal energy potential of heat flow within the Gulf Coastal region (FIG. 9). The thickness of sedimentary units and existing oil and gas wells with large quantities of co-produced fluids make development of an enhanced geothermal system an attractive scenario for the Gulf Coast. Geothermal electrical power production requires high fluid flow rates at temperatures exceeding 100 °C. In areas in Texas, Louisiana, Arkansas, & Mississippi with high heat flow temperatures reach 120 °C in some places at depths of 3 km (~2m) verifying the potential for geothermal resources in the region.

Since the production of this map there has been a significant addition of well data made available by the National Geothermal Database to recreate a thermal depiction of Mississippi. I have combined the SMU and NGDS datasets to develop a higher spatial resolution image of Mississippi to delineate patterns of temperature resources sufficient for future geothermal applications. To achieve this evaluation, I took a more comprehensive approach on estimating thermal conductivity based on composition of five major chronostratigraphic units; the Cenozoic, Upper Cretaceous, Lower Cretaceous, Upper Jurassic, and Paleozoic. This approach adds more detail and provides a significant update to the current estimates of geothermal resources within Mississippi.

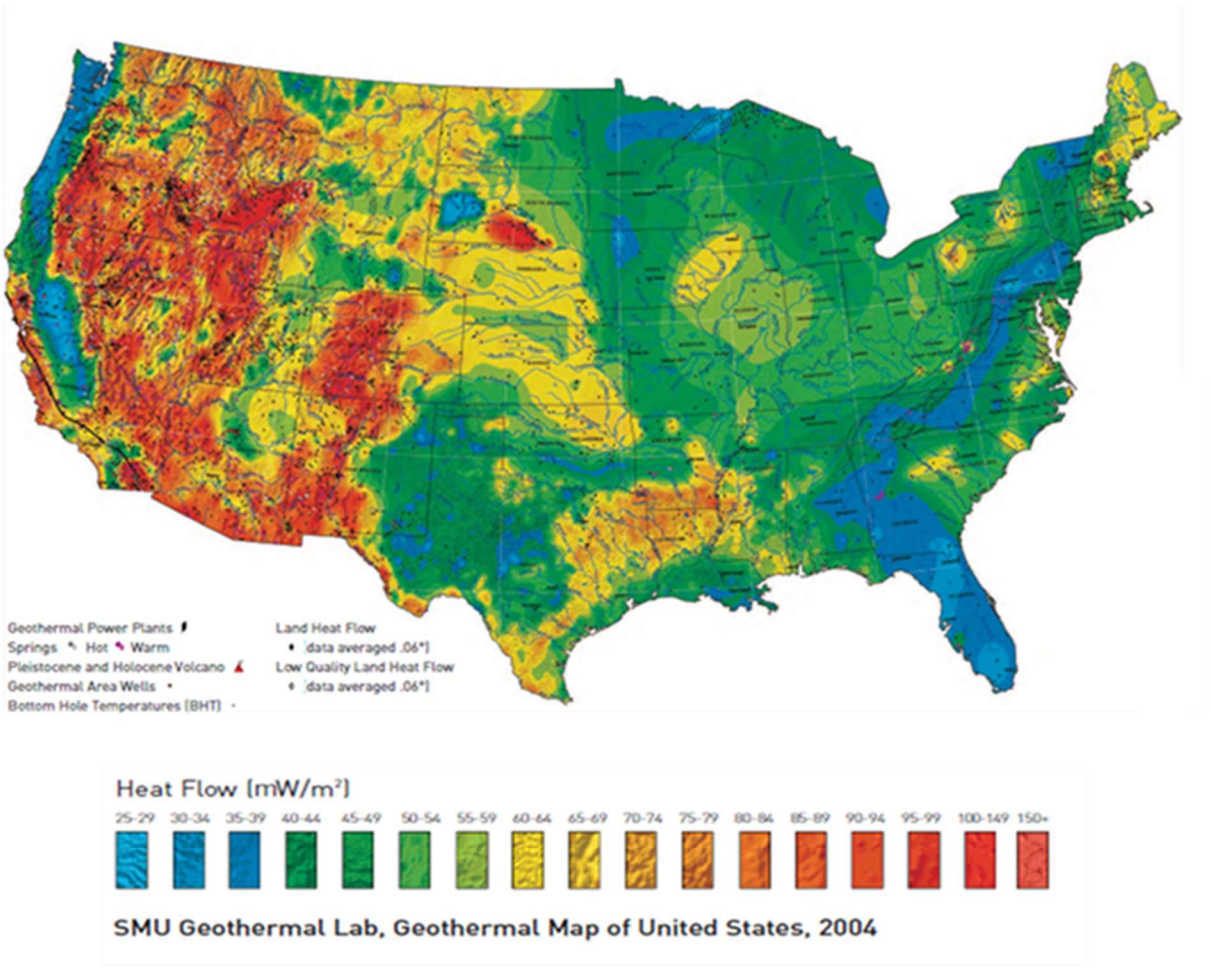

Figure 9 — SMU's conterminous United States heat flow map (Blackwell and Richards, 2004).

CHAPTER 3

MATERIALS AND METHODS

The temperature data used in this assessment consists of the two independent data sets shown in FIG. 10. The Mississippi Department of Environmental Quality (MDEQ), Office of Geology has been collecting and publishing information about the geology and mineral resources of the state since the inception of the Mississippi Geological Survey in 1850. The MDEQ has digitized legacy geothermal relevant data, including borehole temperatures, published existing digital data, and has provided the data online as an accessible database made available for distribution through the National Geothermal Data System (NGDS). This database includes 9,790 wells that were used in the current study.

The second database available is Southern Methodist University (SMU) geothermal laboratory borehole temperature observation. It is a nationwide aggregation of multiple data submissions containing temperature and depth data. It also contains both equilibrium logged measurements and BHT values. This data set is conformant to the content model created by SMU's Geothermal Laboratory in their studies to identify the geothermal potential within the United States. This database includes 937 wells within Mississippi that were used in the current study.

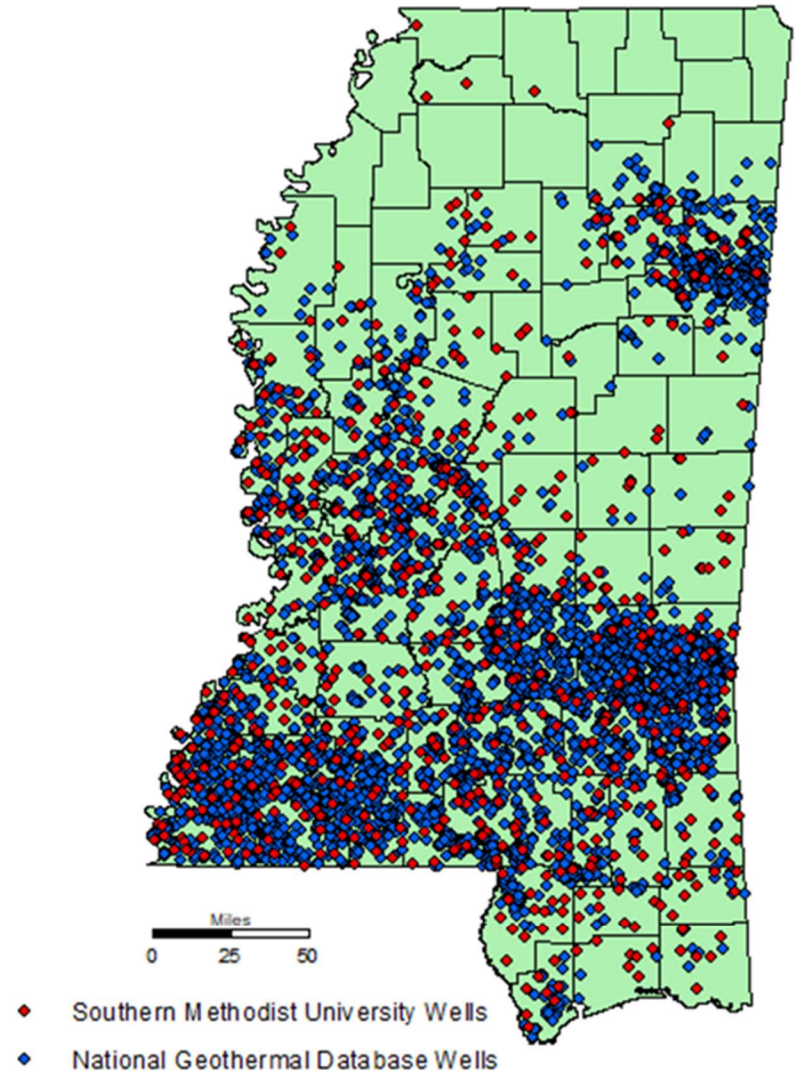

Figure 10 — Locations of different data sets used in this assessment.

The data as obtained from the two sources required review for missing or obviously incorrect values, duplicate records, and anomalous values. Records that were duplicated between the datasets were compared for consistency and duplicates removed from the working data set. Records that were missing any required information (latitude/longitude, well API number, depth, and BHT value) were also removed from the working data set. An initial set of maps using the working data set were generated, and these maps were used to query the datasets and identify anomalous records. Each of these anomalous records were individually reviewed to evaluate whether the data values were reasonably correct or not. Using the Mississippi Oil and Gas Board's online well search application, it was possible to query the original drilling records and identify clerical mistakes made within the datasets. Combination of these two datasets resulted in 7,843 usable records available for this study. The number and depth ranges of wells are shown in FIG. 11.

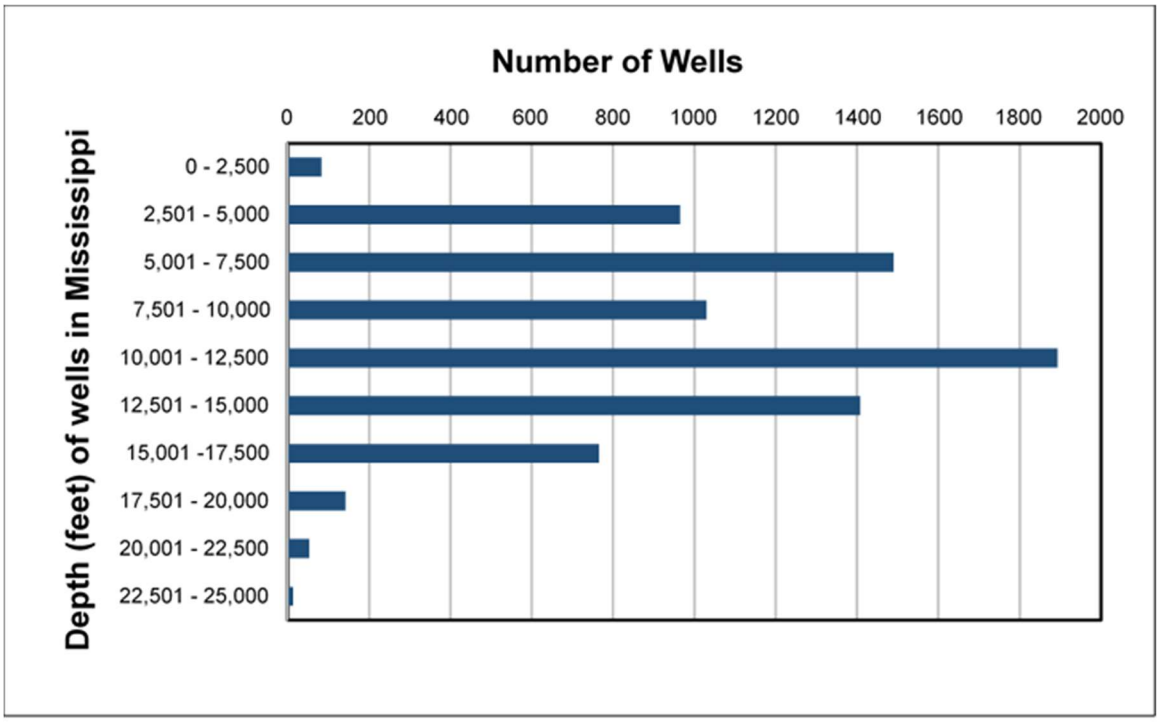

Figure 11 — Histogram of drilling depths versus number of wells used in this study.

Bottom Hole Temperature Correction

During rotary drilling of a petroleum exploration well, fluid is pumped though the drill pipe from the surface to the drill bit to cool the high temperatures created from friction and to act as a high-pressure jet to clean and blast through the rock strata (Blackwell, et al., 2010). This drilling fluid is then transported up the annulus between the borehole and the drill pipe, stabilizing the borehole walls, and resulting in cooling of the borehole at deeper depths and potentially heating it in shallower depths depending on the temperature, drilling speed, and type of drilling fluid. Therefore, in order to measure the correct temperature of strata at depth from a well after the removal of drilling equipment, there needs to be a period of equilibration. Logging of wells usually occurs after initial drilling ceases and before the well section is cased. For wells with multiple casing intervals, this results in; more than one BHT measurement (Blackwell, et al., 2010) at different depths. Only rarely have the borehole temperatures had time to equilibrate and therefore the temperature measurements must be corrected. The best BHT are obtained from pressure tests performed in air drilled gas wells, since the wells do not circulate mud the temperatures are not altered by the fluid. Unfortunately, temperature data collected from air drilled wells are not available for the study area.

The temperature data used in this assessment are from oil and gas wells. There are several different temperature correction formulas that can be applied to estimate the equilibrium temperature of a well from the measured BHT. One of the more commonly used methods for correction of BHT was developed by Harrison et al. (1983). Blackwell and Richards (2004) applied the Harrison correction to the American Association of Petroleum Geologist (AAPG) Geothermal Survey of North America (GSNA) data. They determined that after this correction was applied the results from the corrected logs did not match the data collected from logs of

wells at equilibrium. They proposed a modification to the standard Harrison correction, known as the SMU-Harrison correction. As stated by Dr. David Blackwell and Dr. Maria Richards, in imperial and metric for ease of use, the SMU-Harrison equation is used to correct BHT between depths of 3,000 and 12,900 feet. For wells with BHT measured deeper than 12,900 feet, the BHT data were given a linear increase (or gradient) starting with the maximum value of the SMU-Harrison correction of 33.6°F and increased by 0.05°F every 500 feet. The deeper wells are expected to have longer times between drilling circulation and BHT measurements and therefore the correction gradient does not increase at the same rate as for the shallower depths. The SMU-Harrison Equation, as can be seen from the formula given below, is a second order polynomial that correlates the BHT measurement to depth.

$$\Delta\ ^{\circ}C = -16.51213476 + 0.01826842109\ z - 0.000002344936959\ z^2$$

z = depth in meters.

Geothermal Gradient

Geothermal gradient is the rate of which Earth's temperature increases with depth, which is a result of heat flowing from Earth's warm interior to its surface. On average, away from tectonic plate boundaries, the temperature increases by about 15–30°C (~ 60-85°F) per km of depth within the upper 100 km. The geothermal temperature gradient varies with locality and is typically measured by determining the bottom open-hole temperature after drilling. The rate of increase in temperature with depth can vary considerably with both tectonic setting and the thermal properties of the rock.

Geothermal temperature gradient calculations require both a surface and a bottom hole temperature. Ground surface temperature was estimated using a 30-year mean statewide surface temperature dataset created by researchers at Oregon State University (PRISM Climate Group, 2004). The long-term average dataset is modeled with PRISM using a digital elevation model (DEM) as the predictor grid to assign values to specific areas. Surface temperatures at well locations were added to the SMU and NGDS datasets. BHT values, surface temperature values, and depth of BHT measurements were used to generate an average geothermal gradient for each well.

$$\text{Geothermal Gradient} = \frac{(\text{BHT}) - (\text{Surface Temperature})}{(\text{Depth of Measurement})}$$

The geothermal gradient values assigned to each well point location were converted to a continuous grid with a cell size of 250 meters using inverse distance weighted (IDW) interpolation in ArcGIS 10.5 (FIG. 12). The IDW method interprets the grid (or surface) being generated to be a locationally dependent variable (Phillip, 1982). This method of interpolation assumes that the influence of any measured value on a grid cell decreases as a power (usually 2) of the distance from the sample location but matches each discrete sample location exactly. The IDW grid was then smoothed using a third order polynomial trend surface that represents the gradual trends in the surface over the entire state of Mississippi. Anomalies in the data can be visually pinpointed by subtracting the trend surface raster from the IDW surface raster. This procedure permits identification anomalies above and below the trend surface (FIG. 13). This procedure was used initially to validate the original data sets, and temperature values well outside expected values could be individually evaluated for correct location, depth, and BHT.

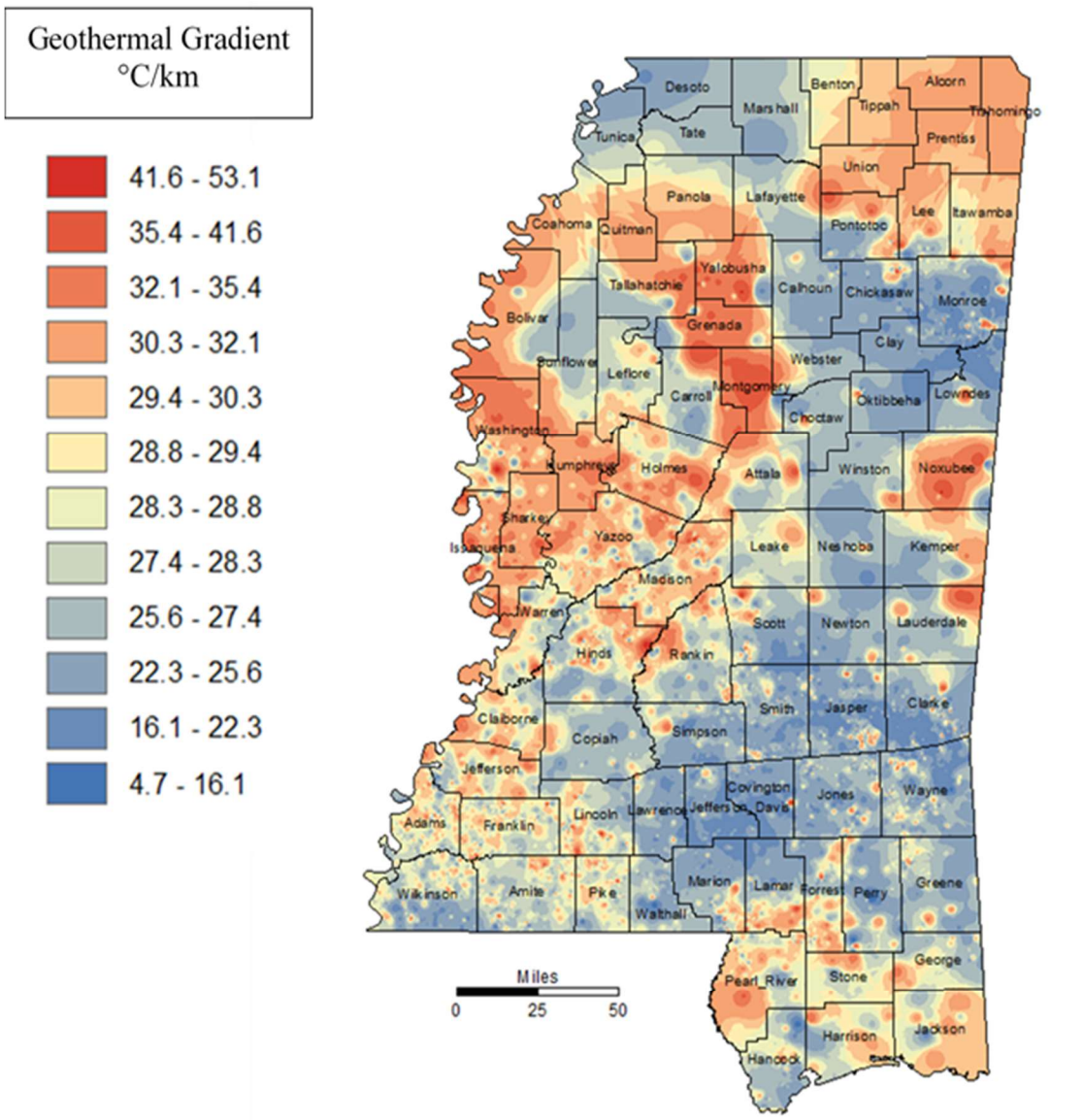

Figure 12 — Geothermal gradient map of Mississippi with a classification method of geometrical interval to provide a better visualization of the continuous data that is not distributed normally.

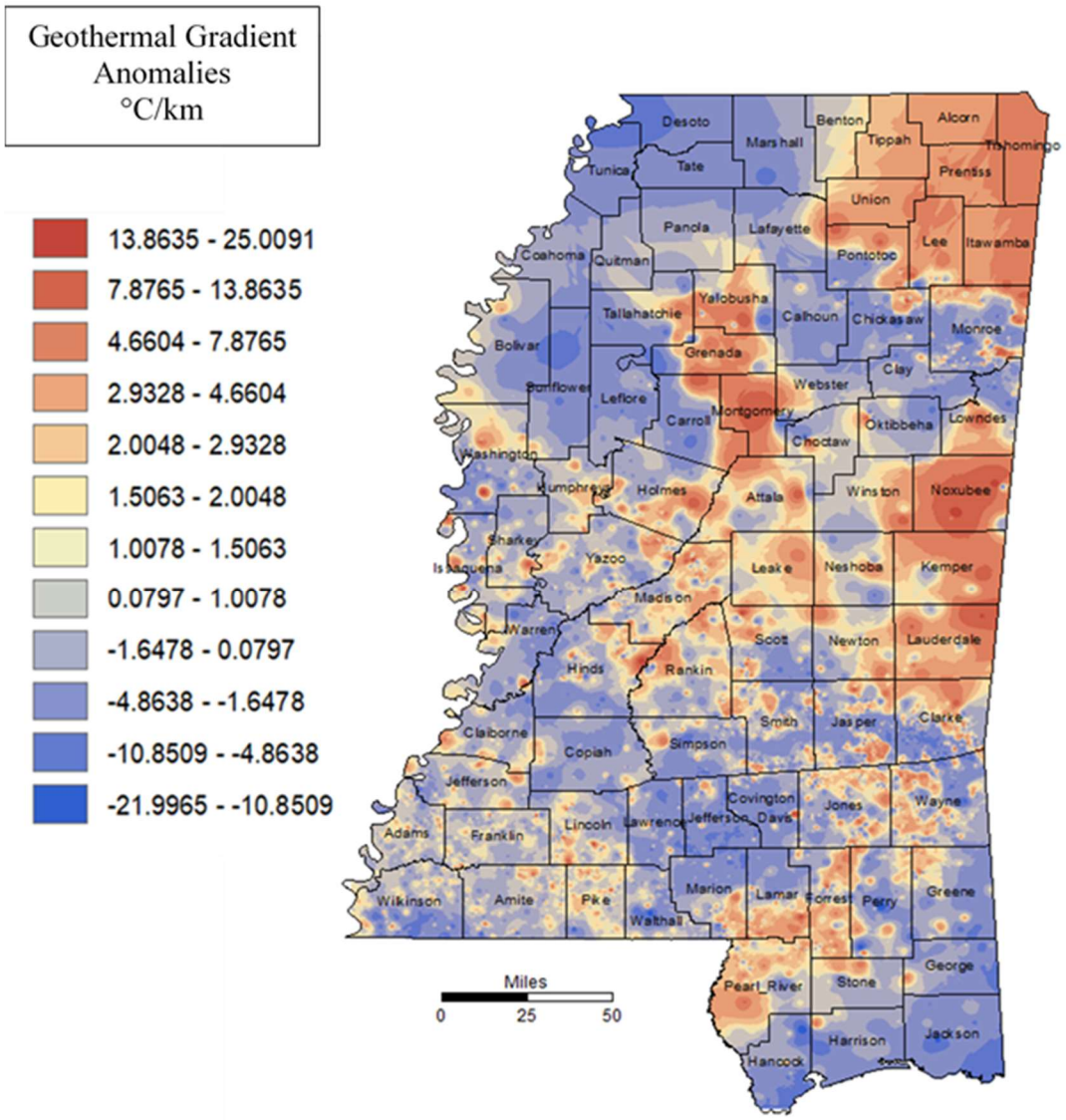

Figure 13 — Geothermal gradient anomalies obtained by subtracting the trend surface raster from the IDW surface raster classified with geometric interval, which was used to identify potential areas of data that need to be investigated for abnormalities.

Geologic Structure

Calculations of the thermal conductivity of rocks underlying Mississippi requires knowledge of the thickness of these rocks, which is in turn calculated from their structural relationships. Estimates of thermal conductivity were made based on characterization of the rock properties of broadly-defined sedimentary rock units. The geologic units chosen to correspond to the depositional chronology of the region and are, in ascending order, (1) Paleozoic formations, (2) Upper Jurassic Formations, (3) Lower Cretaceous formations, (4) Upper Cretaceous formations, and (5) Cenozoic formations. Precambrian rocks are poorly known from the Mississippi area, and, as a result of the Ouachita Orogeny, are likely metamorphosed and have thermal characteristics of the deeper crust and are modeled as crustal basement.

Regional structure maps on each sedimentary unit were generated from, formation tops picked from oil and gas logs, but information for much of the state, particularly for the older formations, was unavailable. In order to supplement well data, structure maps from Dockery & Thompson (2016) and structure maps from Nunnally and Fowler (1954) along with a depth to basement map from Galloway (2008) were digitized and georeferenced. In addition, the depths of geologic unit boundaries were estimated from cross section figures by Dockery (2016 & 2017) and incorporated into the structural models. All data were converted to subsea elevations when necessary. The discrete structural data were then interpolated using the natural neighbor method to create continuous grids of the geologic structure of each sedimentary unit (FIG. 14–18).

The algorithm used by the natural neighbor interpolation tool finds the closest subset of input samples to a query point and applies weights to them based on the proportionate associated areas of influence to interpolate a value (Sibson, 1981). It does not infer trends within the data and does not produce peaks, pits, ridges, or valleys that are not already represented by the input samples. The surface passes through the input samples and is smooth everywhere except at the locations of the input data.

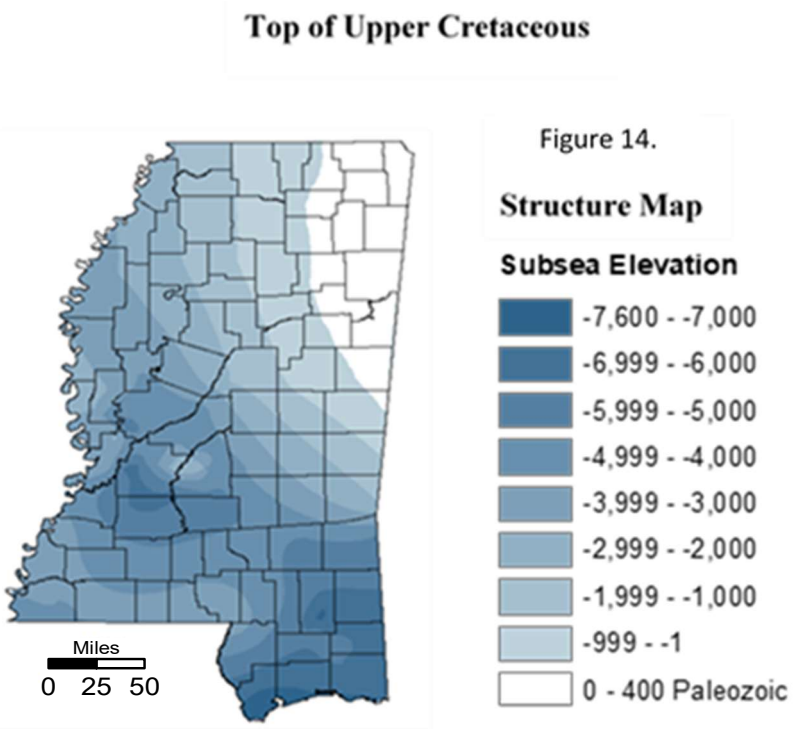

Figure 14.

Top of Lower Cretaceous

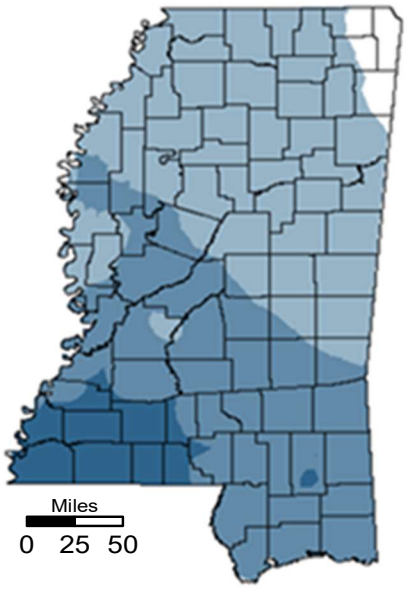

Figure 15.

Structure Map

Subsea Elevation

-14,800 - -10,000
-9,999 - -5,000
-4,999 - -1
0 - 400 Paleozoic

Top of Upper Jurassic

Figure 16.

Structure Map

Subsea Elevation

-24,000 - -20,000
-19,999 - -15,000
-14,999 - -10,000
-9,999 - -5,000
-5000 - 400 Missing Jurassic

Top of Paleozoic

Figure 17.

Structure Map

Subsea Elevation

-39,370 - -30,000
-29,999 - -20,000
-19,999 - -10,000
-9,999 - 0
0 - 400

Top of PreCambrian

Figure 18.

Structure Map

Subsea Elevation

-39,370 - -35,000
-34,999 - -30,000
-29,999 - -25,000
-24,999 - -20,000
-19,999 - -15,000
-14,999 - -10,000
-9,999 - -5,000

Isopach

Isopach maps of the thickness of each of the sedimentary units (FIG. 19–23) were generated from the continuous structure surfaces by subtracting the older surface from the younger in ArcGIS. As a result of tectonics, onlap and erosion, the Cenozoic, Upper Cretaceous, Lower Cretaceous, Upper Jurassic, and Paleozoic sedimentary units are not present or have insignificant thickness in portions of Mississippi. This contingency was managed by using conditional statements to correct the isopach grids for areas where thickness indicates zero.

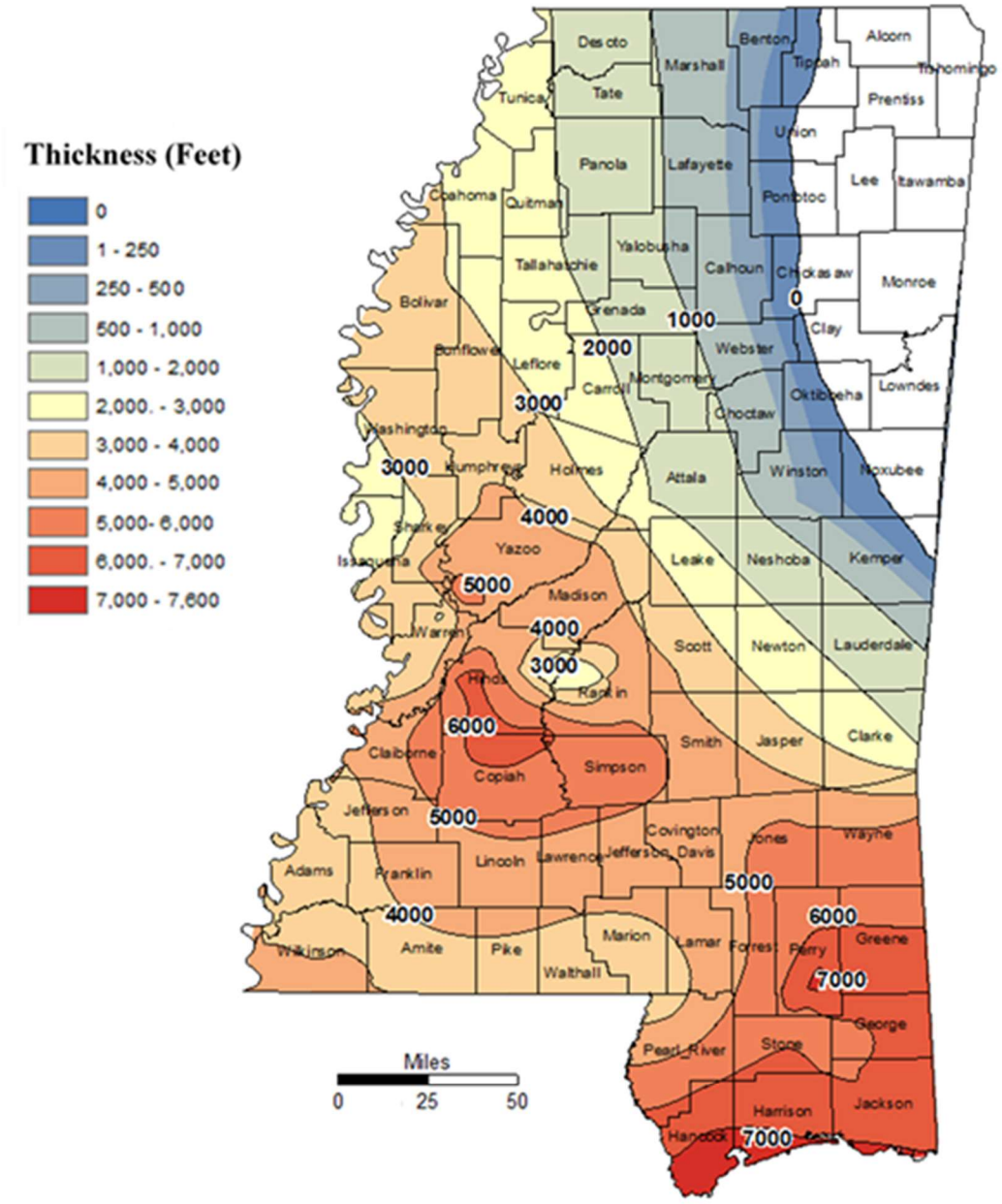

Figure 19 — Cenozoic Isopach map
Contour Interval Upper Right – 250 Feet
Contour Interval – 1000 Feet

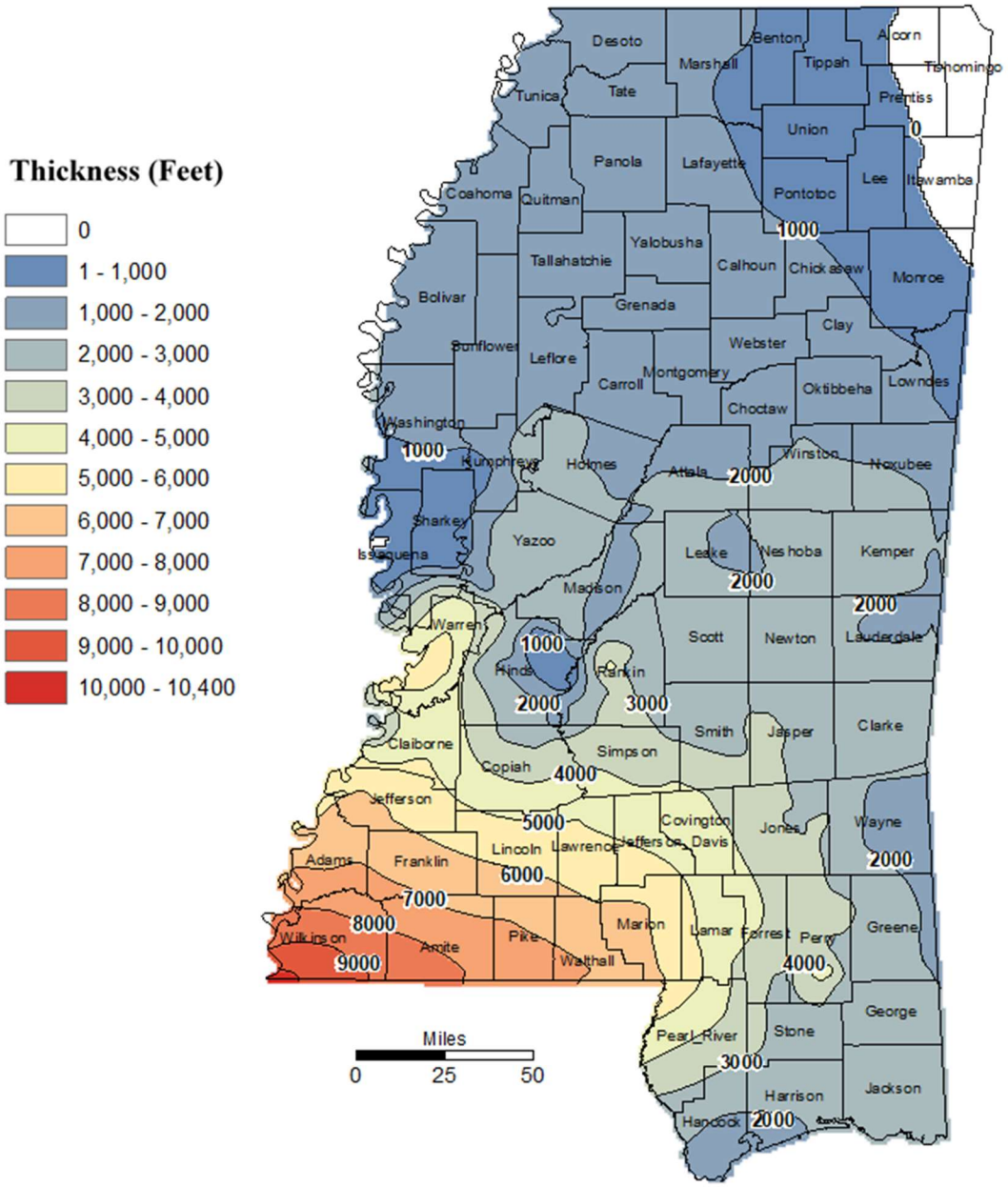

Figure 20 — Upper Cretaceous Isopach map
Contour Interval – 1000 Feet

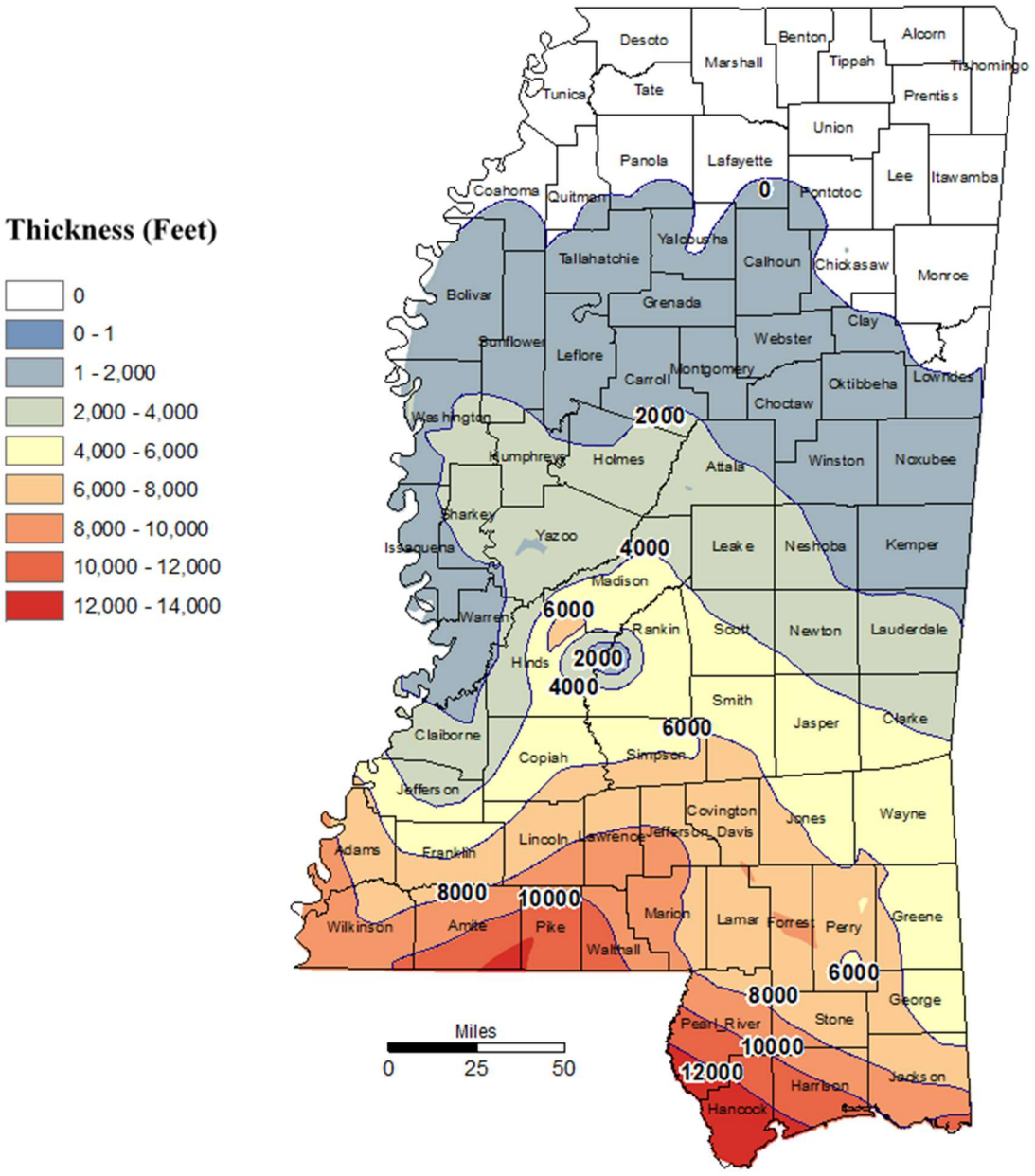

Figure 21 — Lower Cretaceous Isopach map
Contour Interval – 2000 Feet

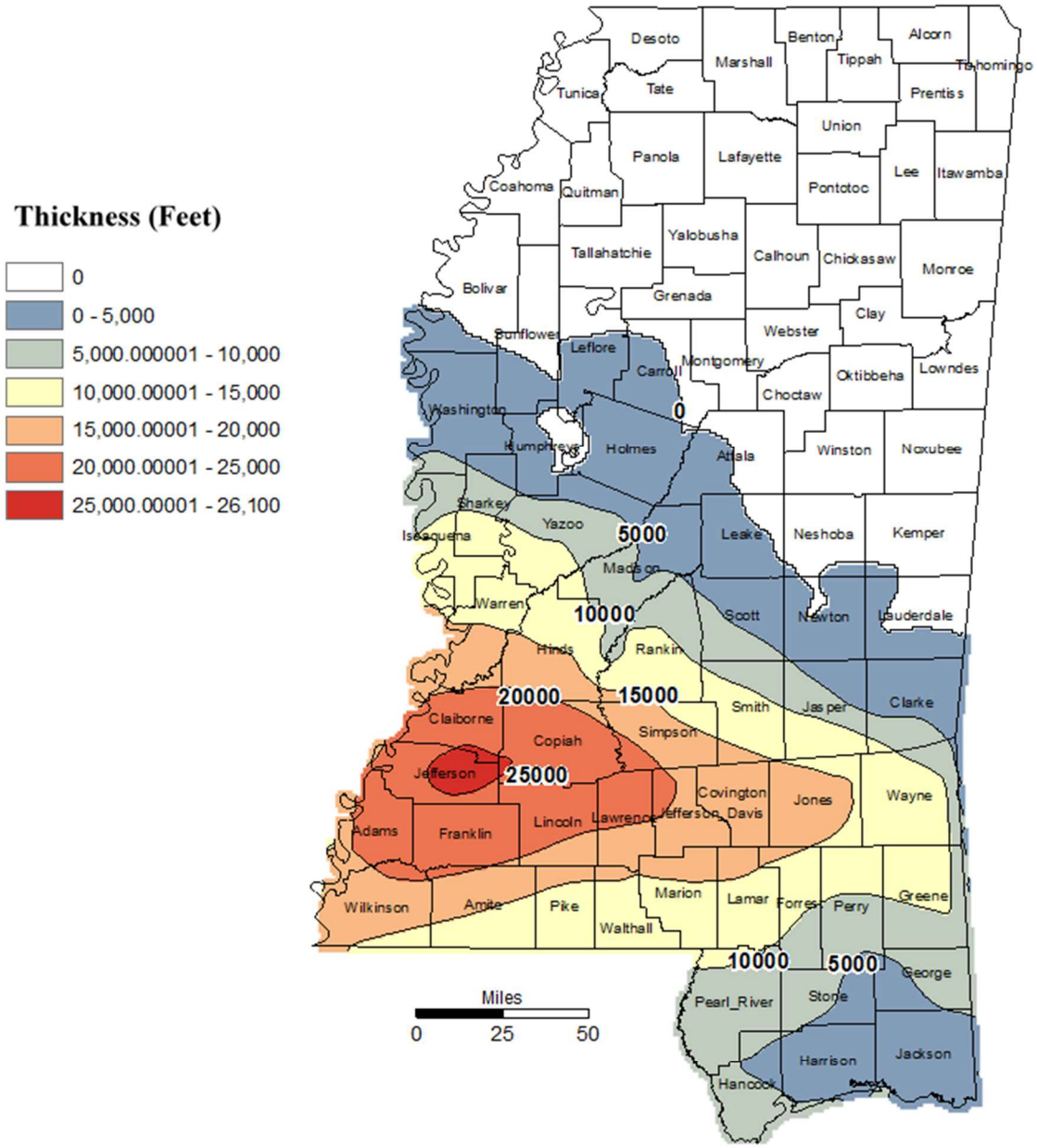

Figure 22 — Upper Jurassic Isopach map
Contour Interval – 5000 Feet

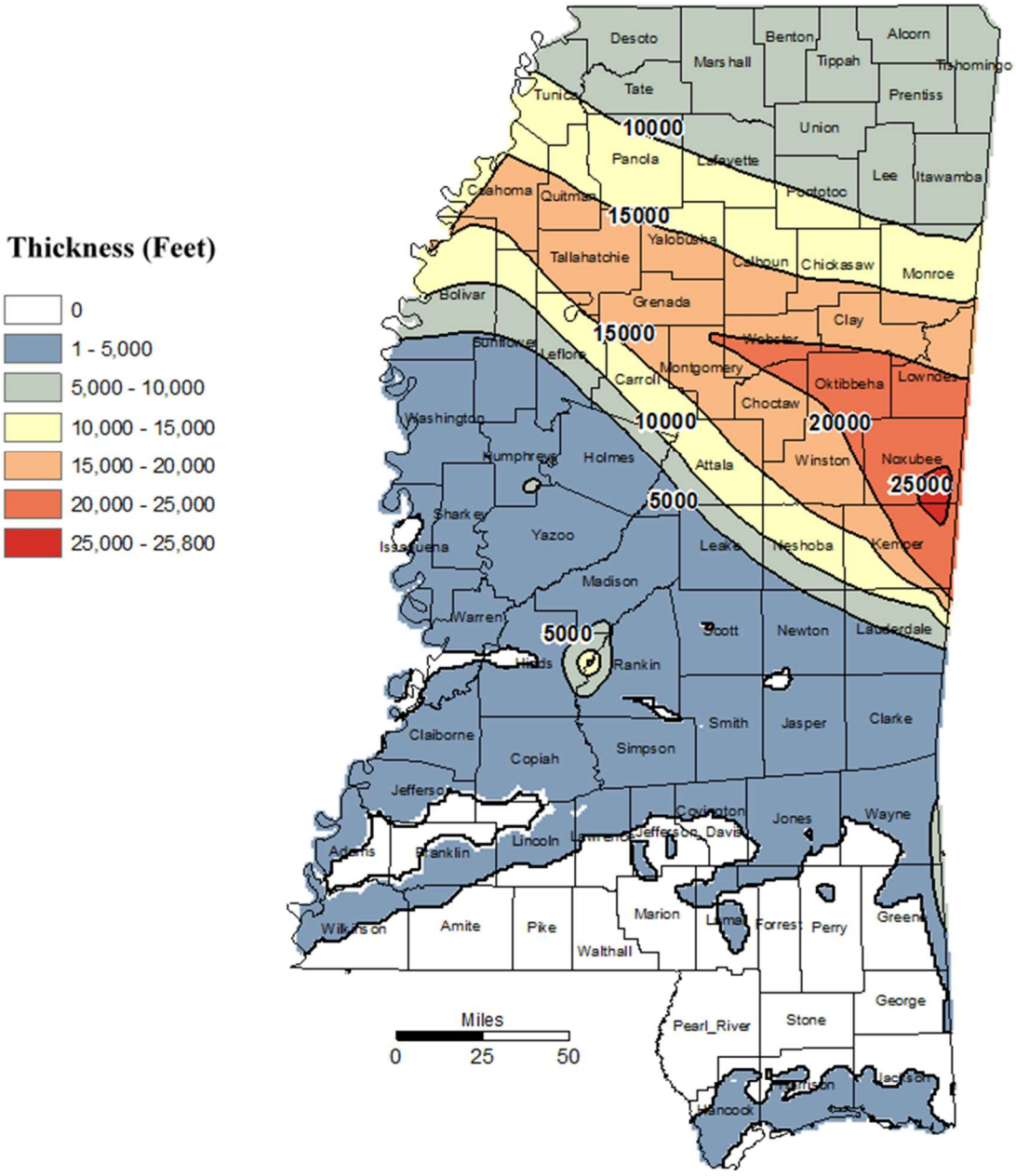

Figure 23 — Paleozoic Isopach map
Contour Interval – 5000 Feet
White Indicates missing Paleozoic

Thermal Conductivity

Thermal conductivity can be determined using rock cores or cuttings on a device that measure the amount of energy the rock sample can transfer. The standard units are typically in watts per meter Kelvin (W/mK or W/m·K) as used here). As can be seen from the formula thermal conductivity values of a rock (mineral) will decrease as the temperature increases. Unfortunately, detailed thermal conductivity data for sedimentary rocks across Mississippi are lacking. For the current study the thermal conductivity measurements will be estimated based on the dominant lithologic composition of Cenozoic, Upper Cretaceous, Lower Cretaceous, Upper Jurassic, and Paleozoic rocks within Mississippi (Dockery, 1997). Thermal conductivities reported by McKenna and Sharp (1998) and Robertson (1988) for sedimentary rocks were used to provide estimates based on primary composition for each time period.

Table 1. Thermal conductivities based on McKenna and Sharp 1998, and Robertson 1988.

Composition	**Thermal Conductivity W/m·K (McKenna, Sharp & Robertson)**
Sandstone	3.8
Limestone	2.8
Shale	2
Salt	5.8

Table 2. Thermal conductivities estimate used based on composition for each sedimentary unit.

Time Interval	Composition	Estimated Thermal Conductivity W/m·K
Cenozoic	Sandstone, Shale, & Limestone	(3.8 + 2.8 + 2) = (8.6/3) = 2.87
Upper Cretaceous	Sandstone & Shale	(3.8 + 2) = (5.8/2) = 2.9
Lower Cretaceous	Sandstone & Shale	(3.8 + 2) = (5.8/2) = 2.9
Upper Jurassic	Limestone & Salt	(2.8 + 5.8) = (8.6/2) = 4.3
Paleozoic	Limestone	2.8

Continuous grids of thermal conductivity were generated from isopach thickness and a averaging formula for conductivity weighted by the lithologic proportions applied of each sedimentary unit. Each thermal conductivity grid could then be multiplied by the geothermal gradient grid to generate a heat flow grid for each time interval. The resulting heat flow grids were then summed to generate a complete heat flow map of Mississippi.

$$WTC\ Cz = ((\ TC_{Cz} * Cz\ Iso) / (Cz\ Iso + UK\ Iso + LK\ Iso + UJ\ Iso + Pz\ Iso))$$

$$WTC\ UK = ((\ TC_{UK} * UK\ Iso) / (Cz\ Iso + UK\ Iso + LK\ Iso + UJ\ Iso + Pz\ Iso))$$

$$WTC\ LK = ((\ TC_{LK} * LK\ Iso) / (Cz\ Iso + UK\ Iso + LK\ Iso + UJ\ Iso + Pz\ Iso))$$

$$WTC\ UJ = ((\ TC_{UJ} * UJ\ Iso) / (Cz\ Iso + UK\ Iso + LK\ Iso + UJ\ Iso + Pz\ Iso))$$

$$WTC\ Pz = ((\ TC_{Pz} * Pz\ Iso) / (Cz\ Iso + UK\ Iso + LK\ Iso + UJ\ Iso + Pz\ Iso))$$

WTC = Weighted Thermal Conductivity
TC = Thermal Conductivity
Iso = Isopach
Cz = Cenozoic
UK = Upper Cretaceous
LK = Lower Cretaceous
UJ = Upper Jurassic
Pz = Paleozoic

CHAPTER 4

RESULTS

Bottom Hole Temperature

After correcting BHT values for both datasets the resulting attributes were exported into Microsoft Excel to generate X, Y scatter plots for further interpretation (FIG. 24-25). This chart shows the relationships between total vertical depth and corrected BHT values. With a high R^2 value of 91% the likelihood of additional well data should fall within the predicted outcome of higher temperatures with deeper wells. Determination does not prove causality and there will always be outliers when it comes to the varying geology of Mississippi.

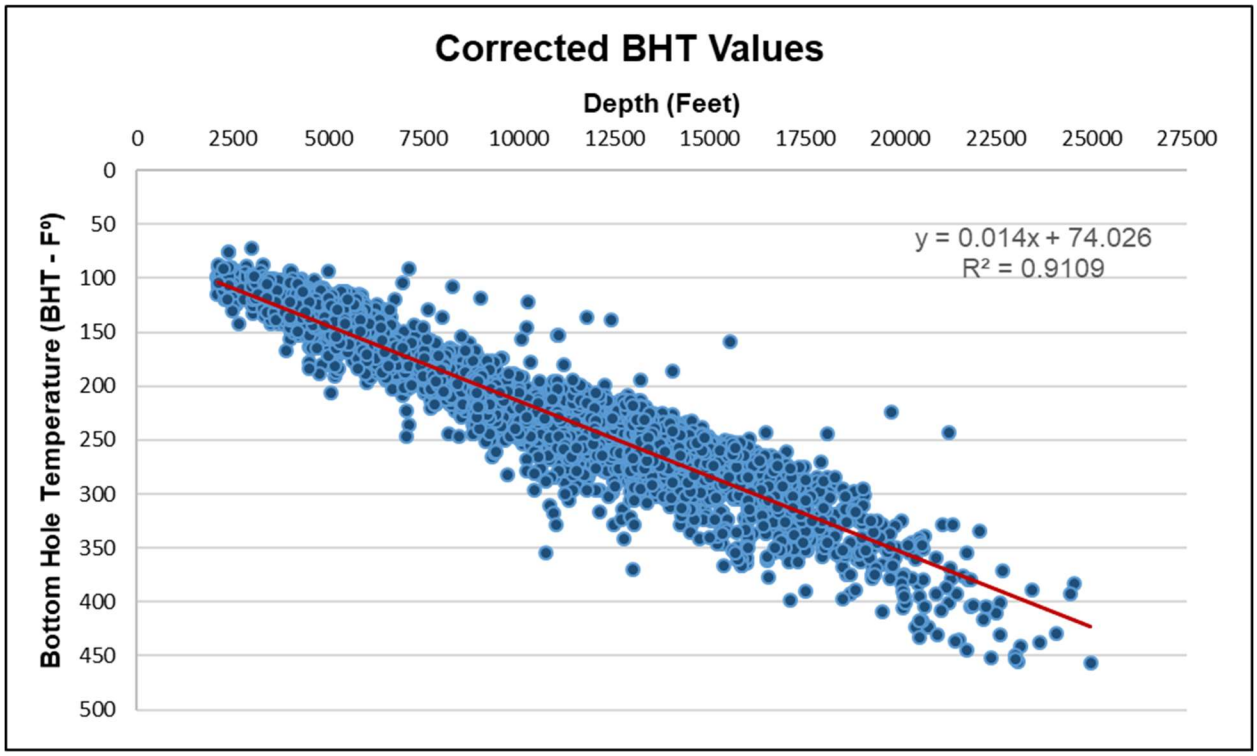

Figure 24 — Scatter plot of wells based on depth versus corrected BHT.values imperial.

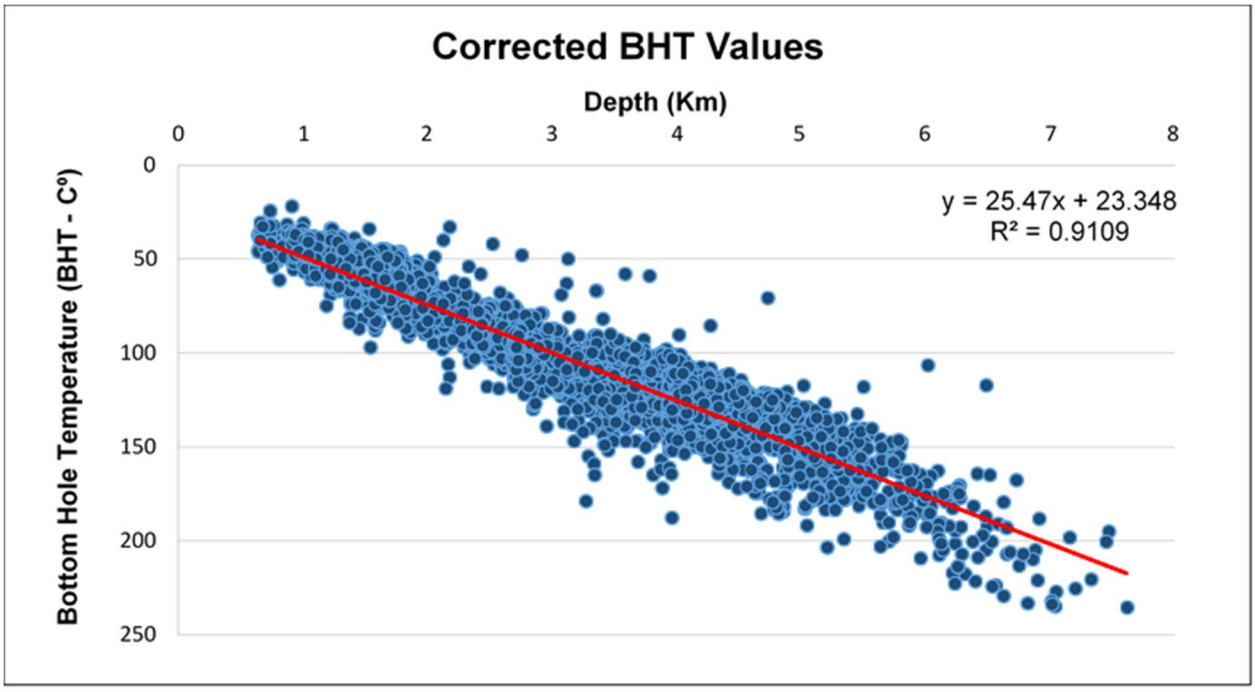

Figure 25 — Scatter plot of wells based on depth versus corrected BHT.values metric.

Absolute Temperature

The scatter plot provides a clear relationship between depth and BHT values, with 4,352 BHT records between 200 – 300°F and 481 BHT records between 300 - 456°F. The wells with highest temperatures above 300°F are grouped mainly within the Mississippi Interior Salt Basin (FIG. 26) with a few outliers that need further investigation to identify the potential heat source.

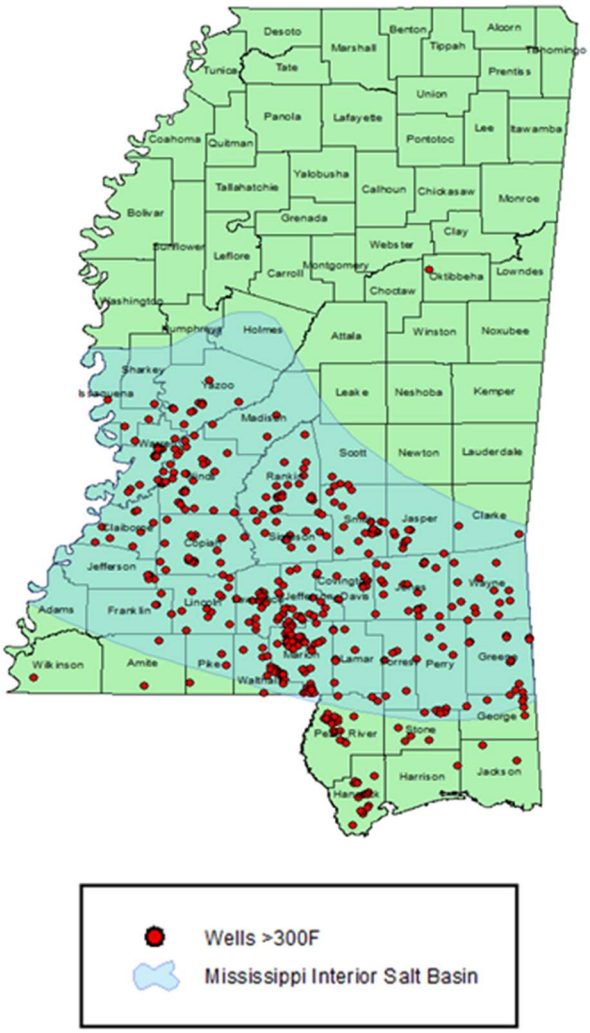

Figure 26 — Wells with temperatures greater than 300°F.

Wells within the 200 - 300°F range are slightly more dispersed, but the majority still lie within the Mississippi Interior Salt Basin (FIG. 27).

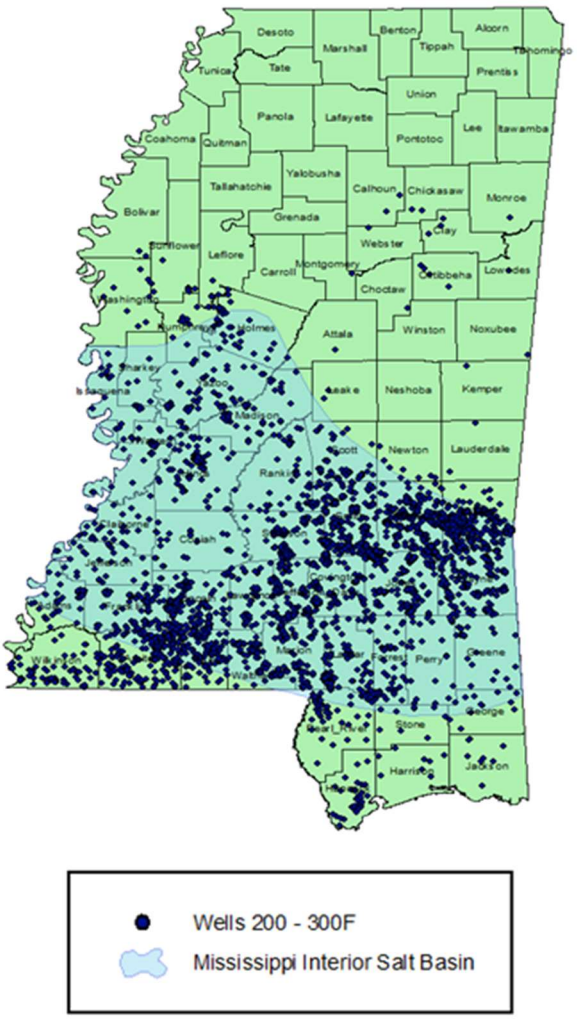

Figure 27 — Wells with temperatures between 200 - 300°F.

Geothermal Gradient

After investigating the geothermal gradient anomalies by cross referencing well data points with Mississippi's Oil and Gas Board I found that anomalous areas were measurements that appeared to be related to depth and temperature of the wells. In some cases, wells were shallow and had abnormally high temperature readings and inversely in deeper wells temperatures were particularly low. This could be caused by several factors including lithology due to thermal conductivity of material or faulting in the area. Only some of these anomalies are due to bad data and as described in methods these were all eliminated. Some anomalous areas of the map correlate to geological features such as salt domes, igneous diapirs, and major structural features that can be seen within the state. This is apparently due to the significant change in geothermal gradient from surrounding areas. With salts high thermal conductivity, the circles present within the MISB indicate dome like structures with a higher geothermal gradient.

In areas surrounding the Jackson Dome and Monroe Uplift a high geothermal gradient is present possibly due to radioactive minerals within the igneous rock as well as heat flow from basement rock. A high geothermal gradient is also present in areas where there are major structural features such as the Wiggins Anticline, Hancock Ridge, buried Ouachita tectonic belt, buried Appalachian belt, and in the northeast Paleozoic rocks. The average statewide geothermal gradient for Mississippi is approximately 27.67 °C/km but in areas where there is high heat flow or high thermal conductivity the gradient can be as high as 53 °C/km. However, in areas where rocks overly potentially pressurized zones geothermal gradient values can be exceptionally low. It is also plausible that upward migration of pore fluid expelled from deep, overpressure zones create areas with a higher thermal gradient.

These geopressured zones can be a important source of localized subsurface heat and can explain (or perhaps be explained by) many features of subsurface structures, including plastic flow of salt, and the development of salt domes/diapirs. Whatever the cause may be higher than normal geothermal gradients are characteristic of Gulf Coast geopressured zones.

Thermal Conductivity

Thermal conductivity grids were created for each stratigraphic interval (FIG. 28-32). These grids show how the material of each interval affects the overall thermal conductivity of the strata. The grids also indicate the extent of how far that stratigraphic interval stretches throughout the state. As a result of tectonics, onlap or erosion, the Cenozoic, Upper Cretaceous, Lower Cretaceous, Upper Jurassic, and Paleozoic sedimentary units are not present or have insignificant thickness in portions of Mississippi. This contingency was managed by using conditional statements to correct the thermal conductivity grids for areas were values indicate zero.

Thermal conductivity values where present appear to correspond with major tectonic features of Mississippi. The Ouachita fold belt is observed in all five intervals providing a clear outline of its magnitude. The high thermal conductivity readings indicate a possible thinning of crust where the belt has risen; as well as the areas associate with the Wiggins and Monroe Uplift. Within the MISB high values of conductivity indicate the abundance of salt known to be part of the Louann Formation. These values provide a clear picture of the influence of tectonic history on geothermal character and were used to generate a new heat flow grid of Mississippi.

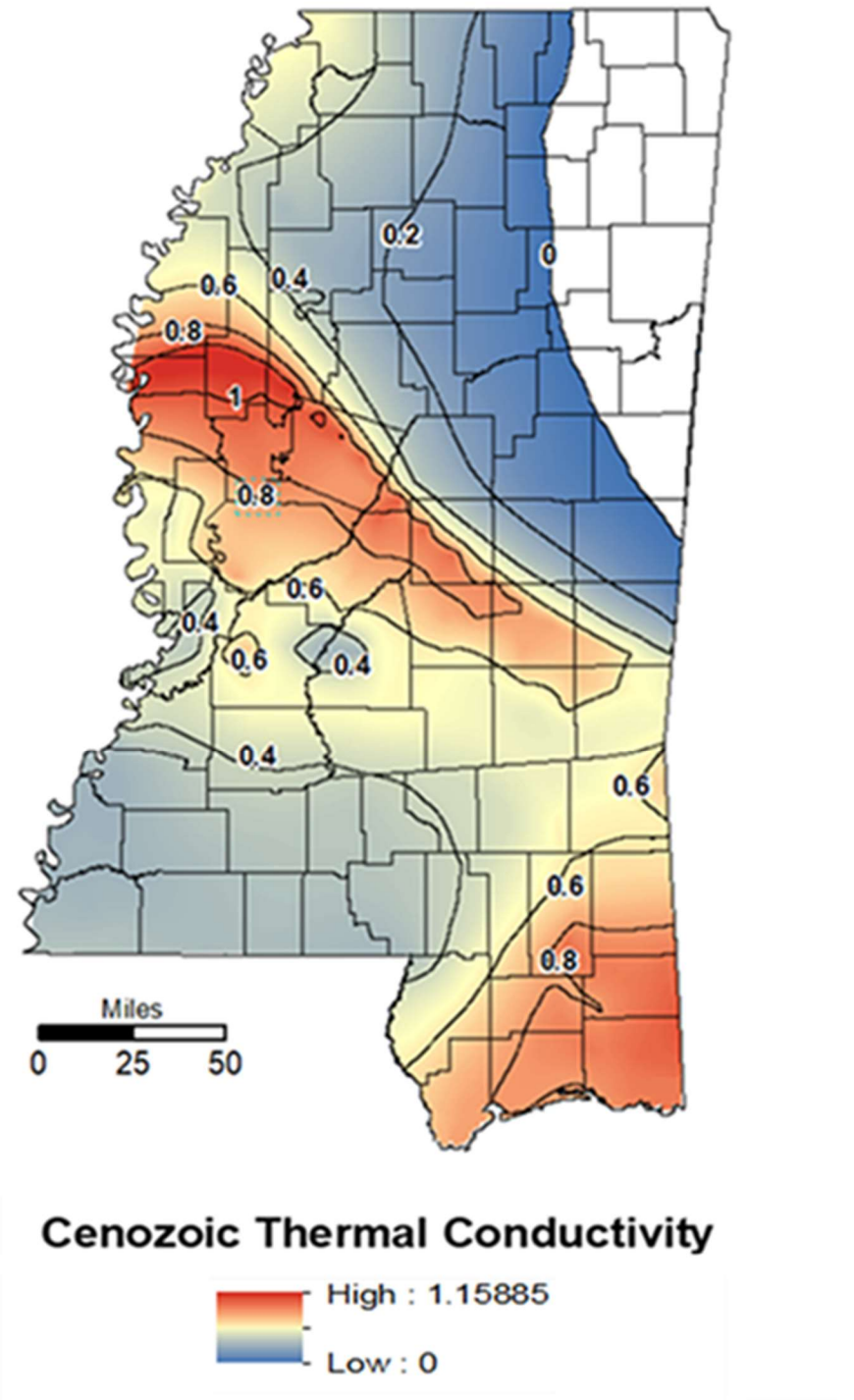

Figure 28 — Thermal conductivity (W/m·K) grid for the Cenozoic interval.

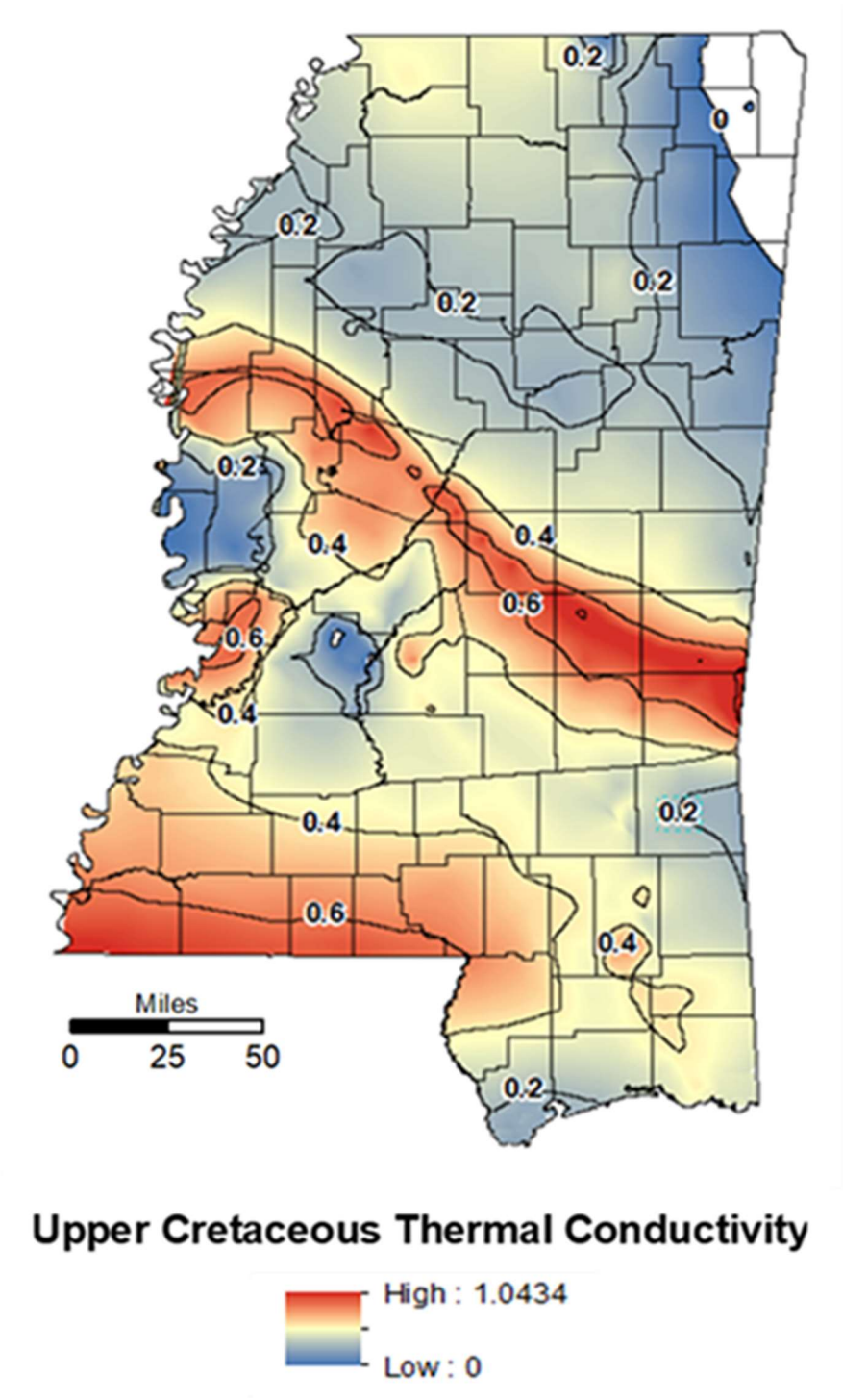

Figure 29 — Thermal conductivity (W/m·K) grid for the Upper Cretaceous interval.

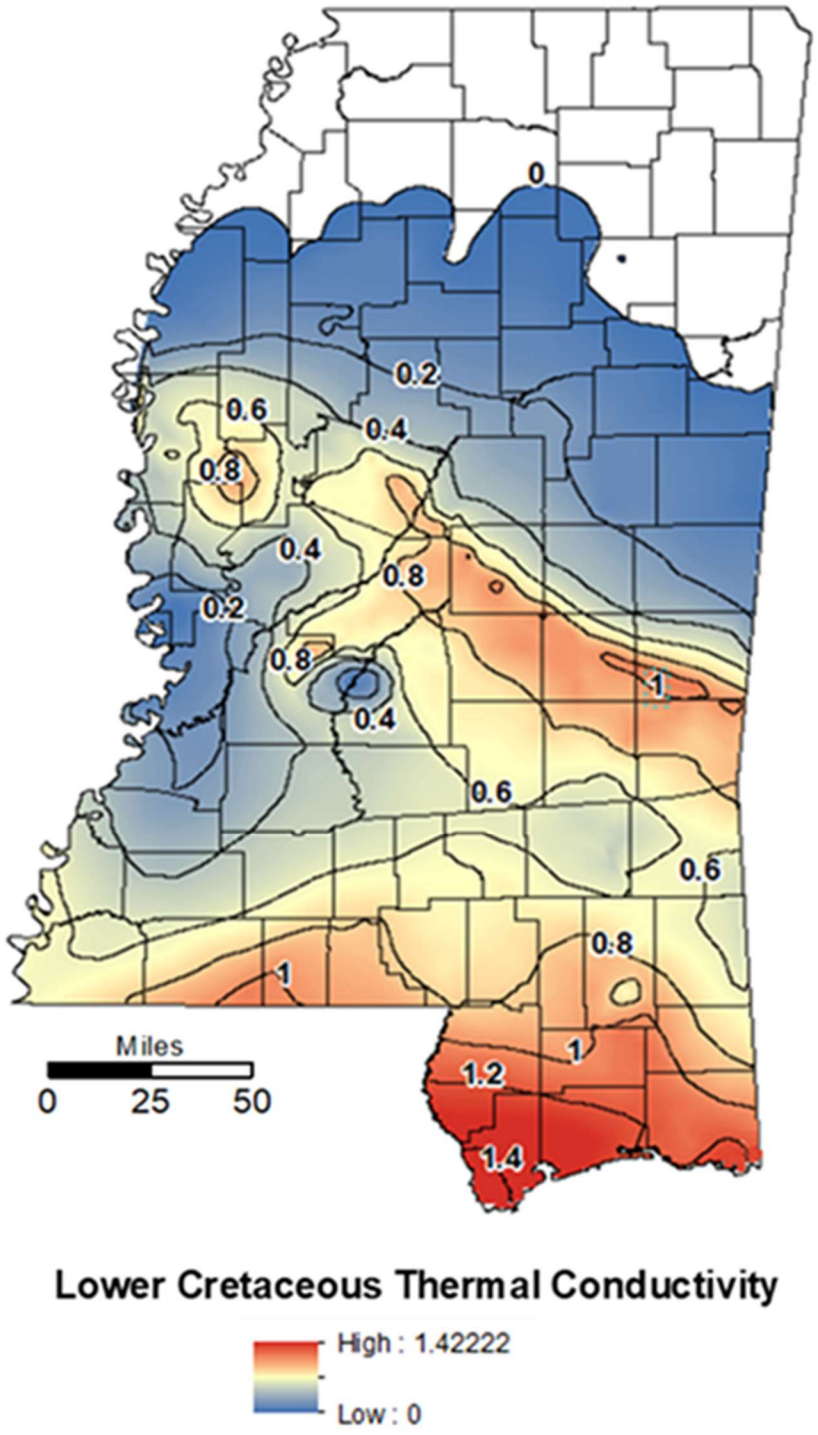

Figure 30 — Thermal conductivity (W/m·K) grid for the Lower Cretaceous interval.

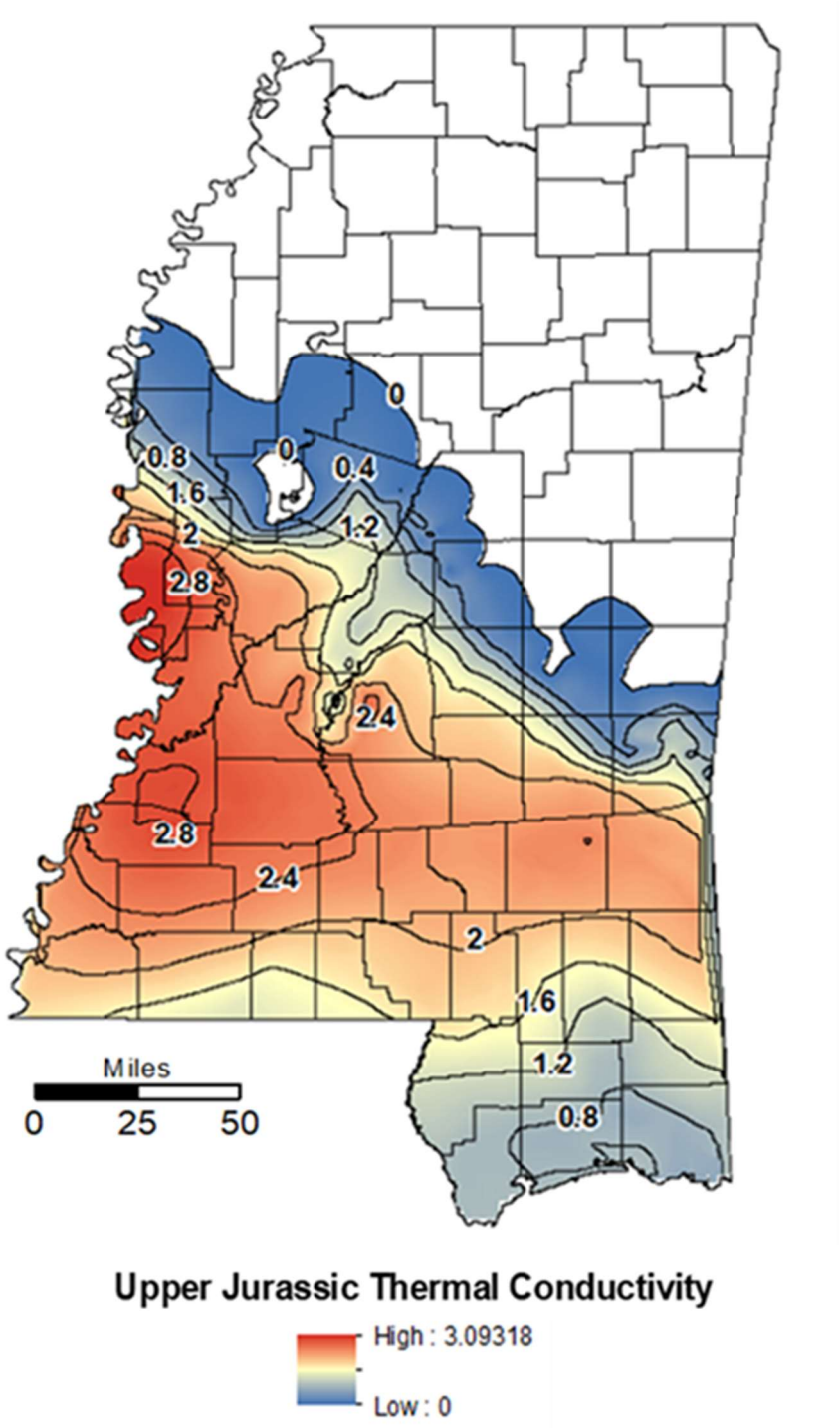

Figure 31 — Thermal conductivity (W/m·K) grid for the Upper Jurassic interval.

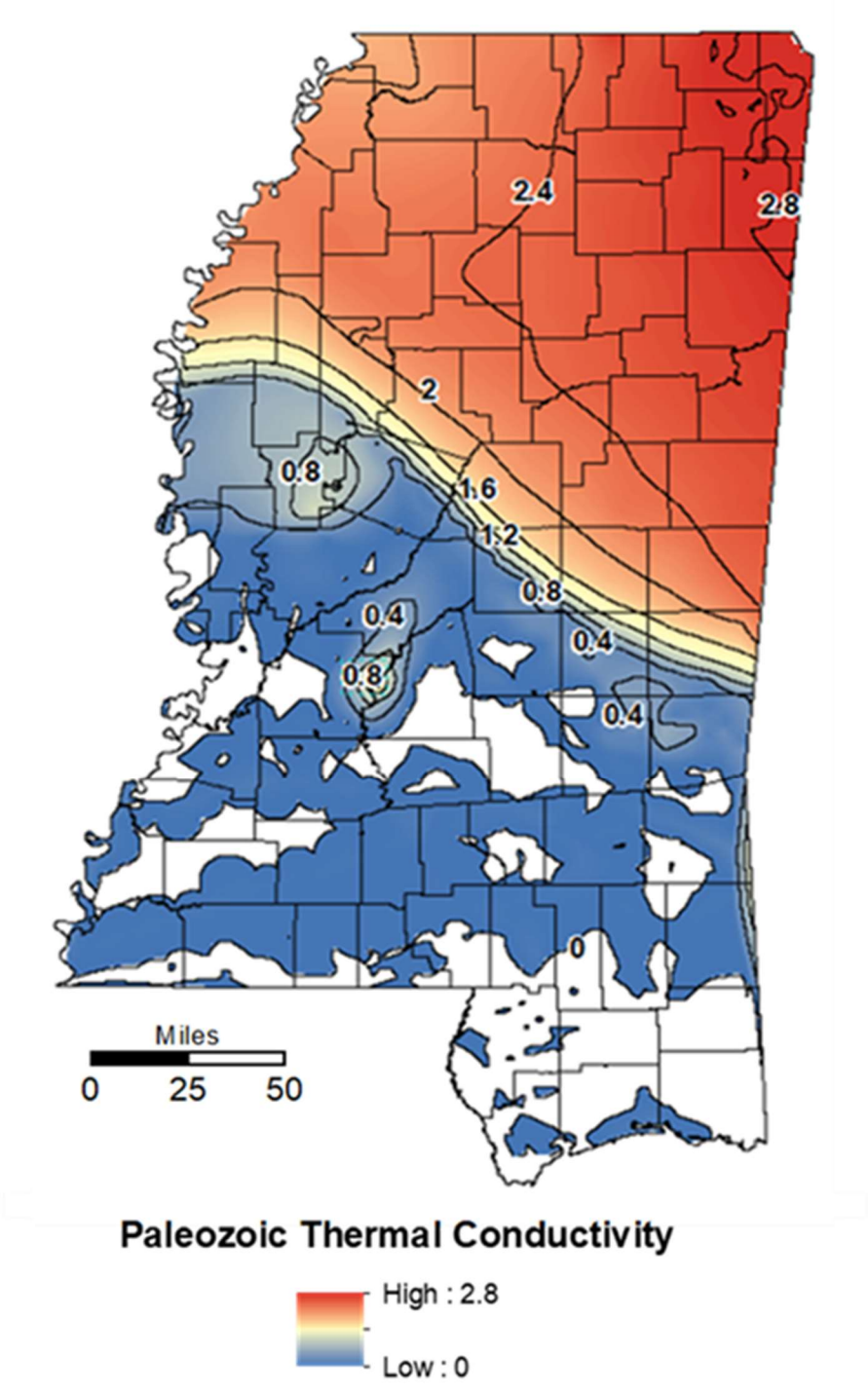

Figure 32 — Thermal conductivity (W/m·K) grid for the Paleozoic interval.

Heat Flow

Previous assessments of geothermal resources have supported the idea that most of the readily recoverable geothermal energy in North America is within the Western United States and the Gulf Coast (Sammel, 1978). A new heat flow evaluation derived from estimated thermal conductivity and geothermal gradient measurements calculated from BHT values and mean surface temperatures indicates that the predominate source of heat flow in Mississippi is mostly contained within the central western portion of the state and within the MISB (FIG. 33). There appears to also be anomalous areas of heat flow above 100 mW/m^2 within the following counties: Washington, Lauderdale, Noxubee, Attala, Lowndes, Grenada, Yalobusha, Pontotoc, Union, Lee, Chickasaw, Wilkinson, Hancock, Harrison, and Jackson.

The array of volcanic features that sprang up in the central region of the Mississippi Embayment during the Late Cretaceous includes the Monroe Uplift, the Sharkey Platform, and the Jackson Dome. The presence of igneous rocks along with the accompanying thinning of crust are most likely the cause of high heat flow measurements in the western central portion of Mississippi. The deep-seated igneous plug known as the Jackson Dome has high potential to be an area for geothermal energy resource. Within the dome heat generated from naturally-occurring radioactive elements is trapped by the overlying sedimentary deposits. Another area associated with high heat flow values is the Louann Formation in the MISB that likely act as a conduit for heat flow due to the salt's high thermal conductivity. These salt bodies represent a superlative medium for geothermal heat conduction, collection, and utilization. Other anomalous areas include the Ouachita trend, Paleozoic outcrops, the Wiggins Uplift, and buried Appalachian mountain belt. Possibly due to a thinning of crust, high radioactive elements within, or excellent conditions for high thermal conductivity.

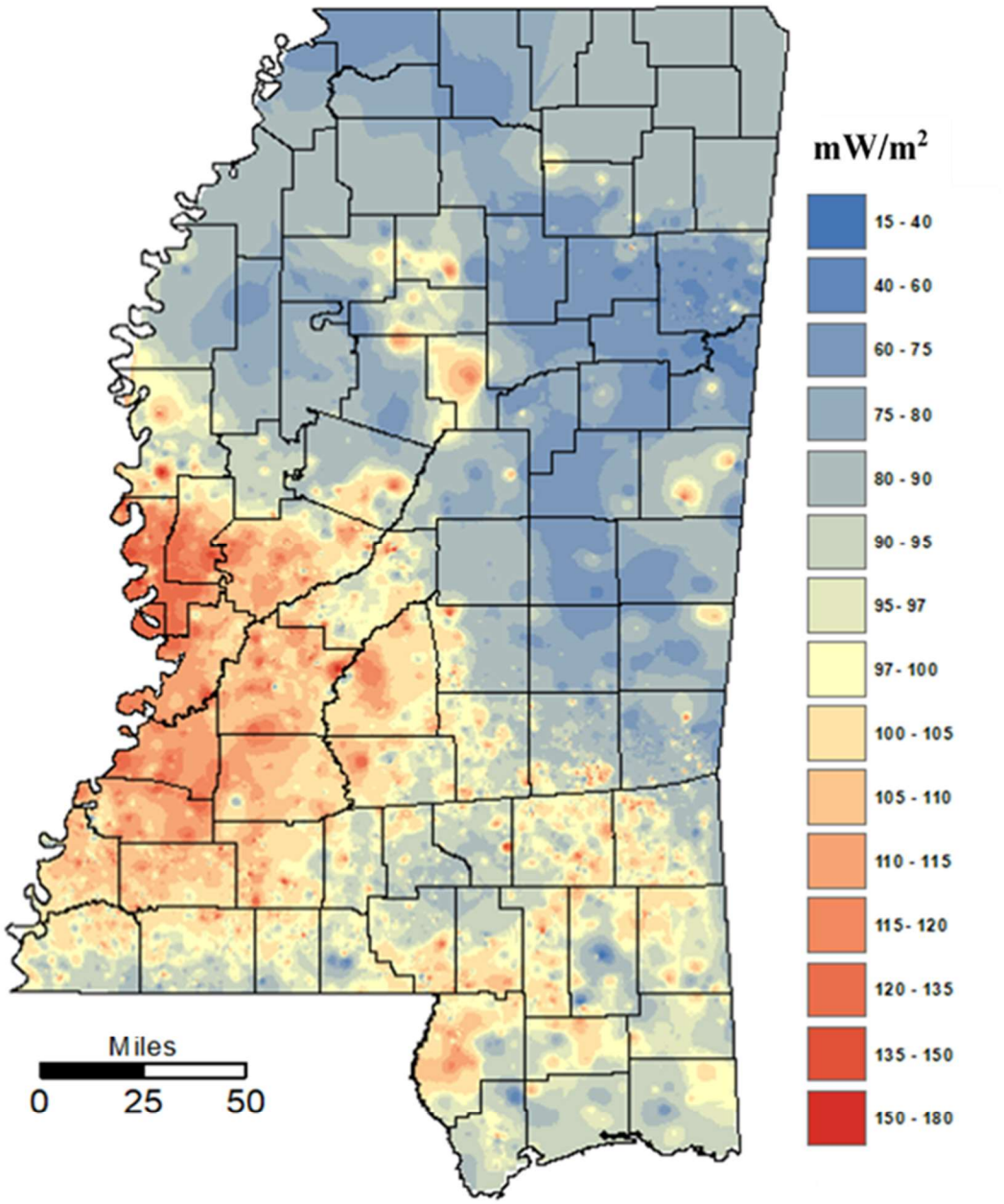

Figure 33 — Heat flow (mW/m^2) of Mississippi based upon estimated thermal conductivity and geothermal gradient.

CHAPTER 5

Conclusion

Along the Gulf Coast undeveloped geothermal energy resources are inferred to exist based on evidence of favorable conditions, such as a high geothermal gradient, thick sequences of low-conductivity sediment, along with geophysical evidence for buried intrusive bodies that may contain radiogenic materials. This study provides comprehensive evidence of such features and several conclusions can be derived from the preparation and interpretation of the heat flow map of Mississippi. BHT values from well logs, if corrected properly, can be a useful tool in mapping geothermal gradients. Major tectonic structural features of Mississippi, such as the interior basin, salt domes, Jackson dome, Ouachita belt, Paleozoic outcrops, Wiggins uplift, and the buried Appalachians are reflected by the geothermal gradient anomalies and trends. However, in areas where rocks overly abnormal pressurized zones geothermal gradient values can be exceptionally low, causing a restriction of heat flow. Estimated intervals of thermal conductivity values based on dominate composition of the strata proved to be an excellent tool in developing heat flow grid for the study area. While only by sampling a chosen location at a desired depth will the actual thermal conductivity values be known, the wealth of data presented here supports the conclusion that significant untapped energy resources are available within the state of Mississippi.

The maps generated in this study show that Mississippi has geothermal energy potential in the central western portion of the state, the MISB, and other anomalous areas near the Ouachita trend and buried Appalachians. These results can be used to easily identify areas of interest with high heat flow that are accessible for further evaluation. Through reservoir engineering and properly managing the resources heat extraction can be maintained over decades. With sedimentary basins and geopressurized formations being an initial entry point for companies to explore, Mississippi's abundance of these key features makes it a prime location for heat extraction. Another way to tap into Mississippi's thermal energy resource is to develop the existing hydrocarbon fields and transform them into geothermal electrical production sites by installing either flash steam power plants or binary power plants depending on the resource temperature. This study indicates a much higher heat flow profile within Mississippi than shown by the SMU 2011 heat flow map of the conterminous United States, especially in the central western portion of the state and within the Mississippi Interior Salt Basin, which is indicative of the additional data and quality assurance procedures used by this study.

List of References

Beckman J. D., Williamson A. K., 1990, Salt Dome Locations in the Gulf Coastal Plain, South-Central United States. Retrieved from https://pubs.usgs.gov/wri/1990/4060/report.pdf.

Blackwell, D., Rachards, M., Frone, Z., Batir, J., Ruzo, A., Dingwall, R., and Williams, M., 2011, Temperature-At-Depth Maps for the Conterminous U. S. and Geothermal Resource Estimates: Geothermal Resources Council Transactions, v. 35, p. 1545–1550.

Blackwell, D., Richards, M., and Stepp, P., 2010, Final Report Texas Geothermal Assessment for the I35 Corridor East Texas State Energy Conservation Office Contract CM709: Texas State Energy Conservation Office Contract CM709.

Brown, D. W., Duchane D.V., Hieken, D. V., & Hriscu, V. T., 2012, Mining the Earth's Heat: Hot Dry Rock Geothermal Energy. In Mining the Earth's Heat (Pg. 17-40), Berlin: Springer.

Department of Energy, A History of Geothermal Energy in America. (N.D.). Retrieved November 27, 2017 from https://www.energy.gov/eere/geothermal/history-geothermal-energy-america.

Department of Energy – Geothermal Technologies Program, 2010, A History of Geothermal Energy Research and Development in the United States: Exploration 1976-2006.

Department of Energy, How an Enhanced Geothermal System Works. (N.D.). Retrieved November 26, 2017 from https://www.energy.gov/eere/geothermal/how-enhanced-geothermal-system-works.

Dockery, D. T., & Thompson, D. E., 2016, The geology of Mississippi. Jackson: University Press of Mississippi.

Dockery, D.T., 1997, Windows into Mississippi's Geologic Past. Jackson: Mississippi Dept. of Environmental Quality, Office of Geology.

Ernest Anderson, D. Hoye Eargle, and B. 0. D., 1973, Geological and Hydrologic Summary of Salt Domes in Gulf Coast Region of Texas, Louisiana, Mississippi, and Alabama. Denver: U.S. Dept. of the Interior, Geological Survey.

Ewing, T. E., 1991, Structural features, in A. Salvador, ed., The Gulf of Mexico Basin: The geology of North America, v. J: Geological Society of America, Boulder, Colorado, p. 31-52.

Galloway W.E., 2008, Depositional Evolution of the Gulf of Mexico Sedimentary Basin. Sedimentary Basins of the World, The Sedimentary Basins of the United States and Canada, p. 505-549.

Harrelson, D.W., and Jennings S.P., 1990, Petrology of a basement core from the Champlin No. 1 International Paper Company Well, Jackson County, Mississippi: Gulf Coast Association of Geological Societies Transactions, v. 41, p. 579.

John Hopkins University. Applied Physics Laboratory, 1978, Geothermal Energy and the Eastern U.S.: The Eastern Gulf Coastal Plain

Kingston, D.R., Dishroon, C.P. & Williams, P.A., 1983, Global basin classification system. American Association of Petroleum Geologists Bulletin, 67, 2175-2193.

Lindsey, C., 2012, Geothermal Energy Potential in Oktibbeha County: Is Mississippi Really Hot? Transactions - Geothermal Resources Council, V. 36 p. 18-21.

Luper, E.E., 1978, An Investigation of Potential Geothermal Energy Sources in Mississippi. Jackson, MS: Mississippi Geological, Economic and Topographical Survey.

Mancini, E.A., Mink, R.M., Bearden, B.L. & Wilkerson, R.P. (1985b) Norphlet Formation (Upper Jurassic) of southwestern and offshore Alabama: environments of deposition and petroleum geology. American Association of Petroleum Geologists Bulletin, 69, 881-898.

Martin, R.G., 1978, Northern and eastern Gulf of Mexico continental margin: stratigraphic and structural framework. American Association of Petroleum Geologists Studies in Geology, 7, 21-42.

Mckenna, T.E., and Sharp, J.M., 1998, Radiogenic Heat Production in Sedimentary Rocks of the Gulf of Mexico Basin, South Texas. Retrieved from https://pubs.er.usgs.gov/publication/70021152.

Mellen, F.F., 1965, Topographical Survey Hinds County Geology and Mineral Resources. Retrieved from https://www.mdeq.ms.gov/geology/work-areas/publications-and-map-sales/categories/bulletins/hinds-county-geology-and-mineral-resources-19378/

Mink, R.M., Tew, B.H., Mann, S.D., Bearden, B.L. & Mancini E.A. (1990) Norphlet and pre-Norphlet geologic framework of Alabama and panhandle Florida coastal waters area and adjacent federal waters area. Geological Survey of Alabama Bulletin 140, p. 58.

Miller, JA, 1982, Structural Control of Jurassic Sedimentation in Alabama and Florida: American Association of Petroleum Geologists Bulletin, v. 66, p. 1289-1301.

Monroe, W.H., 1954, Geology of the Jackson Area Mississippi, Bulletin 986.

Nunnally, J.D., and Fowler, H.F., 1954, Lower Cretaceous Stratigraphy of Mississippi. Mississippi Geological Survey.

Philip, G. M., and D. F. Watson., 1982, "A Precise Method for Determining Contoured Surfaces." Australian Petroleum Exploration Association Journal 22: 205–212.

Pilger, R.H., Jr., 1981, The Opening of the Gulf of Mexico: Implications for the Tectonic Evolution of the Northern Gulf Coast: Transactions of the Gulf Coast Association of Geological Societies, v. 31, p. 377-381.

Pollack, H. N., 1982, The Heat Flow from the Continents. Annual Review of Earth and Planetary Sciences, vol. 10, p. 459-481.

PRISM Climate Group, Oregon State University, http://prism.oregonstate.edu, Retrieved 4 Oct 2018.

Richards, M., 2008, Finding Geothermal Energy in Texas. Retrieved from https://www.smu.edu/-/media/Site/Dedman/Academics/Programs/Geothermal-Lab/Documents/TeacherMaterials/SMU-_Teachers_Geothermal_Resource_projects.pdf?la=en.

Robertson, E.C., 1988, Thermal Properties of Rocks: US Department of the Interior: Geological Survey, p. 88–441.

Salvador, A, 1987, Late Triassic-Jurassic Paleogeography and Origin of Gulf of Mexico Basin: American Association of Petroleum Geologists Bulletin, v. 71, p. 419-451.

Sammel E.A., 1978, Occurrence of low-temperature geothermal waters in the United States. Retrieved from https://pubs.usgs.gov/circ/1979/0790/report.pdf.

Sawyer, D.S., Buffler, R.T. & Pilger, R.H., Jr., 1991, The crust under the Gulf of Mexico. In the Gulf of Mexico Basin (Ed. by A. Salvador, Geological Society of America, Decade of North American Geology, J, 53-72.

Setterfield B., 2015, Salt Dome Analysis, Retrieved from http://www.setterfield.org/salt_deposits/salt_dome_analysis_text.html

Sibson, R., 1981, “A Brief Description of Natural Neighbor Interpolation," chapter 2 in Interpolating Multivariate Data. New York: John Wiley & Sons, p. 21–36.

Smith, D.L., and Dees, W.T., 1982. Heat Flow in the Gulf Coastal Plain. Jour. Geophvs. Res. 87, pp 7687-76939.

Winker, C. N. and Buffler, R.T., 1988, Paleogeographic Evolution of Early Deep-Water Gulf of Mexico and Margins, Jurassic to Middle Cretaceous (Cenomanian): American Association of Petroleum Geologists Bulletin, v. 72, p. 318- 346.

Wood, M.L. & Walper, J.L. (1974) The evolution of the interior Mesozoic basin and the Gulf of Mexico. Transactions Gulf Coast Association of Geological Societies, 24, 31-41.

Yurewicz, D.A., Marler, T.B., Meyreholts, K.A., & Siroky, F.X. (1993) Early Cretaceous carbonate platform, north rim of the Gulf of Mexico, Mississippi and Louisiana. In: Cretaceous Carbonate Platforms (Ed. by J.A.T. Simo, R.W. Scott, and J.P. Masse), Association of Petroleum Geologists Memoir 56, 81-96.

APPENDIX

Cenozoic points used to create the natural neighbor raster

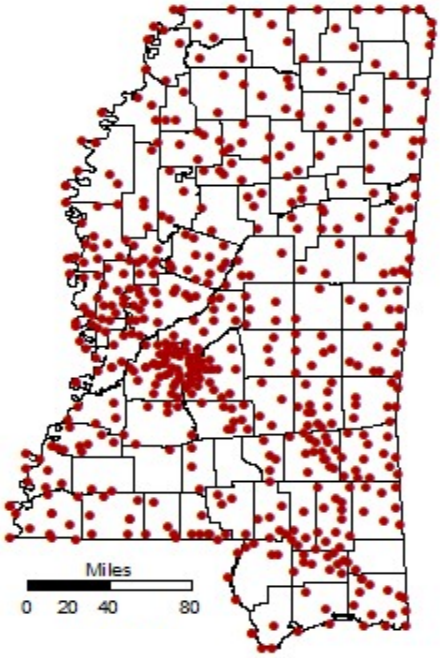

Upper Cretaceous points used to create the natural neighbor raster

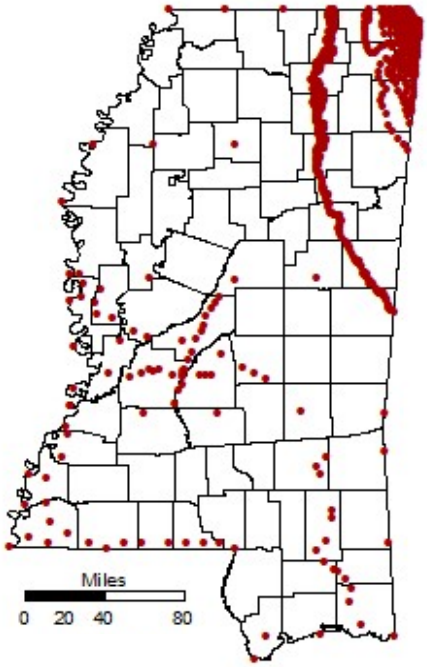

Lower Cretaceous points used to create the natural neighbor raster

Upper Jurassic points used to create the natural neighbor raster

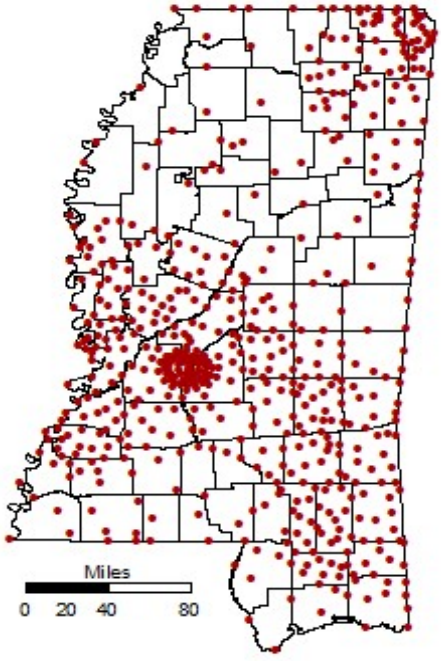

Paleozoic points used to create the natural neighbor raster

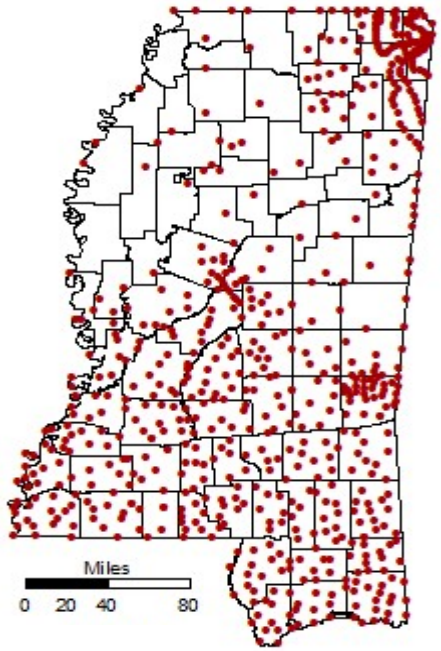

Precambrian points used to create the natural neighbor raster

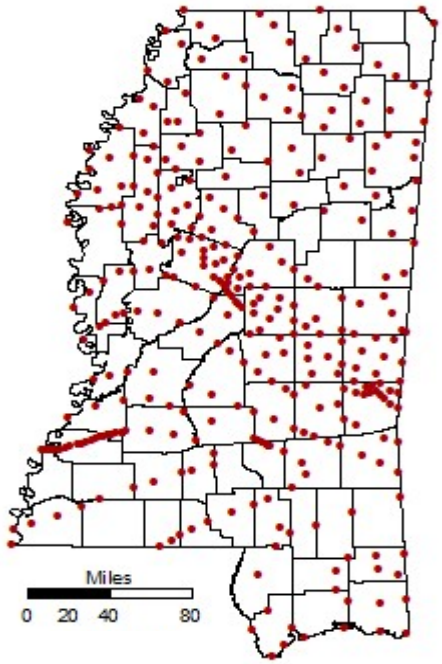

Salt Domes in Mississippi

OBJECTID	Dome Name	County	Latitude	Longitude	Depth to Salt
1	Allen	COPIAH	31.79	-90.64	-2774
2	Arm	LAWRENCE	31.52	-90.02	-1930
3	Brownsville	HINDS	32.47	-90.39	-4689
4	Bruinsburg	CLAIBORNE	31.93	-91.13	-2016
5	Burns	SMITH	32.12	-89.56	-11310
6	Byrd	GREENE	31.23	-88.68	-2058
7	Carmicheal	HINDS	32.08	-90.48	-2966
8	Carson	JEFERSON DAVIS	31.6	-89.77	-3086
9	Caseyville	LINCOLN	31.67	-90.68	-3035
10	Centerville	JONES	31.7	-89.34	-2400
11	County Line	GREENE	31.43	-88.52	-1343
12	Cypress Creek	PERRY	31.14	-88.96	-1190
13	D'Lo	SIMPSON	32.03	-89.89	-2250
14	Dont	COVINGTON	31.72	-89.45	-2200
15	Dry Creek	COVINGTON	31.65	-89.71	-2100
16	Eagle Bend	WARREN	32.55	-90.99	-4425
17	Edwards	HINDS	32.31	-90.54	-3026
18	Ellisville	JONES	31.61	-89.16	-14075
19	Eminence	COVINGTON	31.63	-89.41	-2440
20	Eucutta	WAYNE	31.79	-88.83	-11804
21	Galloway	CLAIBORNE	32.07	-90.93	-4432
22	Glass	WARREN	32.21	-90.97	-4030
23	Glazier	PERRY	31.33	-88.9	-7685
24	Grange	JEFFERSON DAVIS	31.68	-89.95	-15274
25	Gwinville	JEFFERSON DAVIS	31.68	-89.84	-10000
26	Halifax	HINDS	32.49	-90.56	-4000
27	Hazelhurst	COPIAH	31.93	-90.29	-1850
28	Heidelberg	JASPER	31.87	-89.02	-9390
29	Hervey	CLAIBORNE	31.85	-90.74	-3547
30	Hiwanee	WAYNE	31.85	-88.57	-13598

31	Kings	WARREN	32.41	-90.81	-3845
32	Kola	COVINGTON	31.66	-89.5	-3048
33	Lampton	MARION	31.22	-89.72	-1647
34	Laurel	JONES	31.69	-89.16	-12304
35	Learned	HINDS	32.22	-90.57	-4437
36	Leedo	JEFFERSON	31.66	-90.87	-2065
37	McBrlde	JEFFERSON	31.76	-90.81	-2205
38	McLaurln	FORREST	31.13	-89.28	-1933
39	Midway	LAMAR	31.29	-89.51	-2205
40	Montlcello	LAURENCE	31.54	-90.17	-2757
41	Moselle	JONES	31.53	-89.32	-2200
42	New Home	SMITH	31.87	-89.33	-2595
43	Nevman	WARREN	32.21	-90.78	-5108
44	Oak Ridge	WARREN	32.45	-90.72	-5062
45	Oakley	HINDS	32.24	-90.48	-2634
46	Oakvale	JEFFERSON DAVIS	31.46	-89.94	-2696
47	Ovett	JONES	31.49	-89.13	-13156
48	Petal	FORREST	31.4	-89.26	-1739
49	Prentlss	JEFFERSON DAVIS	31.58	-89.88	-2800
50	Raleigh	SMITH	31.96	-89.5	-2140
51	Richmond	COVINGTON	31.49	-89.54	-1954
52	Rlchton	PERRY	31.36	-88.95	-722
53	Rufus	RANKIN	32.15	-89.78	-12485
54	Ruth	LINCOLN	31.4	-90.3	-2700
55	Sardls Church	COPIAH	31.82	-90.32	-2000
56	Sunrise	FORREST	31.35	-89.2	-5940
57	Tatum	LAMAR	31.16	-89.56	-1516
58	Utlca	COPIAB	32.01	-90.61	-3135
59	Valley Park	SHARKEY	32.67	-90.89	-12424
60	Vlcksburg	WARREN	32.35	-90.89	-4386
61	Wesson	COPIAH	31.72	-90.38	-3550
62	Yellow Creek	WAYNE	31.78	-88.62	-11422
63	Bethel	ANDERSON	31.89	-95.93	-1600
64	Boggy Creek	ANDERSON	31.97	-95.42	-1829
65	Brooks	SMITH	32.17	-95.45	-220
66	Brushy Creek	ANDERSON	31.91	-95.61	-3570

67	Bullard	SMITH	32.17	-95.29	-527
68	Butler	FREESTONE	31.67	-95.86	-312
69	Concord	ANDERSON	31.91	-95.69	-6000
70	East Tyler	SMITH	32.37	-95.25	-890
71	Elkhart	ANDERSON	31.59	-95.63	-10165
72	Girlie Calduell	SMITH	32.28	-95.4	-6002
73	Grand Saline	VAN ZANDT	32.66	-95.69	-213
74	Halnesville	WOOD	32.7	-95.36	-1155
75	Keechi	ANDERSON	31.85	-95.7	-300
76	La Rue	HENDERSON	32.16	-95.66	-4450
77	Marquez	LEON	31.23	-96.26	-613
78	Mount Sylvan	SMITH	32.38	-95.44	-800
79	Oakwood	FREESTONE	31.56	-95.95	-122
80	Palestine	ANDERSON	31.74	-95.73	-10200
81	S Locum	ANDERSON	31.63	-95.52	-300
82	Steen	SMITH	32.52	-95.31	-535
83	Whltehouse	SMITH	32.23	-95.28	-1324
84	Alien	BRAZORIA	28.94	-95.52	-3929
85	Arrlola	HARDIN	30.24	-94.24	-1000
86	Barbers Hill	CHAMBERS	29.85	-94.87	-2050
87	Big Creek	FORT BEND	29.49	-95.74	-635
88	BLg Hill	JEFFERSON	29.76	-94.25	-1300
89	BLue RLdge	FORT BEND	29.58	-95.48	-230
90	Bollng	UHARTON	29.3	-95.91	-975
91	Brenham	WASHINGTON	30.09	-96.45	-1136
92	Bryan Mound	BRAZORIA	28.93	-95.36	-1100
93	Cedar Point	CHAMBERS	29.64	-94.92	-10231
94	Clam Lake	JEFFERSON	29.72	-94.1	-8173
95	Clay Creek	WASHINGTON	30.34	-96.37	-2400
96	Clemens	BRAZORIA	28.99	-95.55	-1380
97	Damon Mound	BRAZORIA	29.29	-95.72	-529
98	Danbury	BRAZORIA	29.26	-95.31	-4948
99	DavLs HL1L	LIBERTY	30.33	-94.84	-1200
100	Day	MADISON	30.97	-95.94	-3167
101	Esperson	LIBERTY	29.95	-94.92	-6170
102	Fannett	JEFFERSON	29.87	-94.25	-2080

103	Fergusons Crossing	BRAZOS	30.61	-96.15	-3757
104	Gulf	MATAGORDA	28.72	-95.87	-1100
105	Hankatner	LIBERTY	29.89	-94.58	-7582
106	Hawkinsvllle	MATAGORDA	28.92	-95.65	-450
107	High Island	GALVESTON	29.58	-94.38	-1228
108	Hockley	HARRIS	29.96	-95.83	-1010
109	Hoskins Mound	BRAZORIA	29.16	-95.21	-1100
110	Hull	LIBERTY	30.11	-94.62	-595
111	Humble	HARRIS	29.99	-95.23	-1214
112	Klttrell	HOUSTON	31.03	-95.47	-3855
113	Long Point	FORT BEND	29.39	-95.71	-868
114	Lost Lake	CHAMBERS	29.84	-94.75	-5430
115	Manvel	BRAZORIA	29.49	-95.31	-11274
116	Markham	MATAGORDA	29	-96.13	-1417
117	Mllllcan	BRAZOS	30.49	-96.21	-5170
118	Moss Bluff	CHAMBERS	29.9	-94.67	-1077
119	Mykawa	HARRIS	29.61	-95.29	-7100
120	Nash	FORT BEND	29.32	-95.63	-950
121	North Dayton	LIBERTY	30.09	-94.98	-800
122	Orange	ORANGE	30.06	-93.84	-7120
123	Orchard	FORT BEND	29.58	-95.95	-369
124	Pierce Junction	HARRIS	29.64	-95.39	-860
125	Pott Neches	ORANGE	30.04	-93.93	-6948
126	Racoon Bend	WALLER	29.79	-96	-11004
127	Red Fish Reef	CHAMBERS	29.52	-94.87	-15228
128	San Fellpe	AUSTIN	29.99	-96.07	-4755
129	Saratoga	HARDIN	30.3	-94.5	-1900
130	Sour Lake	HARDIN	30.16	-94.4	-719
131	South Houston	HARRIS	29.67	-95.23	-4386
132	South Liberty	LIBERTY	30	-94.82	-480
133	Spindle Top	JEFFERSON	30.03	-94.07	-1200
134	Stratton Ridge	BRAZORIA	29.05	-95.33	-1250
135	SugarLand	FORT BEND	29.54	-95.56	-4280
136	Thompson	FORT BEND	29.45	-95.57	-9320
137	Webster	HARRIS	29.57	-95.16	-10430
138	West Columbia	BRAZORIA	29.17	-95.64	-768

139	144 Galveston Block	Unknown	29.29	-94.53	-1741
140	MBea	Unknown	29.58	-94.2	-2605
141	SLPa	Unknown	29.04	-95.05	-358
142	SBea	Unknown	29.32	-94.71	-2640
143	DRan	MC MULLEN	28.47	-98.64	-7645
144	Palf	ST BROOKS	27.17	-98.12	-1140
145	Moca	ST WEBB	27.86	-98.83	-6366
146	Pala	ST DUVAL	27.7	-98.41	-500
147	Pesc	ST WEBB	27.59	-99.3	-14400
148	PPln	ST DUVAL	27.6	-98.39	-1205

Geodatabase Directory

Backup Folder

Annotations.gdb – Editable geological features of Mississippi
- Anticlines - Line
- Intrusions - Line
- Synclines - Line
- Mississippi Interior Salt Basin - Polygon
- Editable Polygon - Polygon

Basemap.gdb – General basemap information along with Prism surface temperatures
- Administrative - Point
- Boundaries - Line
- Transportation - Line
- Weather – Point & Line
- Prism 30-year MSTM – Raster Dataset

Contours.gdb – Contours of each stratigraphic interval used
- Cenozoic Contour 1000 Ft 2 - Line
- Upper Cretaceous Contour 1000 Ft 2 - Line
- Lower Cretaceous Contour 1000 Ft 2 - Line
- Upper Jurassic Contour – 5000 Ft 3 - Line
- Paleozoic Contour - Line

Geology.gdb – Editable geological features of Mississippi
- Salt Domes - Point
- Structure Points - Point
- Salt Domes Table File
- Salt Domes Depth Table

Geothermal Gradient.gdb – Geothermal Gradient rasters used
- Geothermal Gradient C/Km Clip – Raster Dataset
- Geothermal Gradient C/Km IDW Clip – Raster Dataset
- Geothermal Gradient C/Km Trend2 – Raster Dataset
- Geothermal Gradient K/m – Raster Dataset
- Geothermal Gradient K/m Clip – Raster Dataset

Heat Flow.gdb – Heat flow rasters used
- Cenozoic Heat Flow4 – Raster Dataset
- UpCretaceous Heat Flow3 – Raster Dataset
- LoCretaceous Heat Flow3 – Raster Dataset
- UpJurassic Heat Flow3 – Raster Dataset
- Paleozoic Heat Flow3 – Raster Dataset
- Heat Flow W/m·K Updated – Raster Dataset
- Heat Flow mW/m^2 Updated Smooth – Raster Dataset

IDW Interpolations.gdb

Isopach Maps.gdb – Isopach maps generated
- Cenozoic Isopach – Raster Dataset
- Cenozoic Isopach Con – Raster Dataset
- Cenozoic Isopach Con Smooth – Raster Dataset
- UpCretaceous Isopach 8 – Raster Dataset
- UpCretaceous Isopach 8 Smoothed – Raster Dataset
- UpCretaceous Isopach 8 Smoothed Con – Raster Dataset
- LoCretaceous Isopach 2 – Raster Dataset
- LoCretaceous Isopach 2 Con2 - Gr– Raster Dataset id
- LoCretaceous Isopach 2 Con2 Smooth – Raster Dataset
- UpJurassic Isopach 6 – Raster Dataset
- UpJurassic Isopach 6 Con4 – Raster Dataset
- UpJurassic Isopach 6 Con4 Smooth – Raster Dataset
- Paleozoic Isopach 5 – Raster Dataset
- Paleozoic Isopach 5 Con Smooth – Raster Dataset
- Paleozoic Isopach 5 Smoothed – Raster Dataset

MsGeol.gdb – Geology of Mississippi
- Placemarks - Polygon
- Cenozoic Units - Polygon
- Mesozoic Units - Polygon
- Paleozoic Units - Polygon
- MS Geol Boundaries - Polygon
- MS Geology - Polygon

Natural Neighbor Interpolation – Structure rasters used
- Cenozoic NatNeigh – Raster Dataset
- Cenozoic NatNeigh Clip – Raster Dataset
- Mesozoic UpCret NatNeigh7 – Raster Dataset
- Mesozoic UpCret NatNeigh7 Clip – Raster Dataset

Mesozoic LoCret NatNeigh5 – Raster Dataset
Mesozoic LoCret NatNeigh5 Clip – Raster Dataset
Mesozoic UpJurr NatNeigh 2 – Raster Dataset
Mesozoic UpJurr NatNeigh 2 Clip – Raster Dataset
Paleozoic NatNeigh 4 – Raster Dataset
Paleozoic NatNeigh 4 Clip – Raster Dataset
PreCambrian Basement NatNeigh – Raster Dataset
PreCambrian Basement NatNeigh Clip – Raster Dataset

Scanned Maps.gdb – Maps used for georeferencing
Base of Lower Cretaceous – Raster Dataset
Galloway 2008 – Raster Dataset
Structural Features – Raster Dataset
Top of Jurassic – Raster Dataset
Top of Lower Cretaceous – Raster Dataset
Top of Paleozoic – Raster Dataset

Thermal Conductivity.gdb – Thermal conductivity rasters used
Cenozoic TC – Raster Dataset
Cenozoic TC Contour3 - Line
UpCretacecous TC – Raster Dataset
Upper Cretaceous TC Contour - Line
LoCretaceous TC – Raster Dataset
Lower Cretaceous TC Contour - Line
UpJurassic TC2 – Raster Dataset
Upper Jurassic TC Contour - Line
Paleozoic TC – Raster Dataset
Paleozoic TC Contour - Line

Wells.gdb – Well data from NGDS and SMU
Basement Wells - Point
Combo Wells - Point
NGD Wells Dockery - Point
SMU Wells - Point
Updated NGD Wells - Point
Updated SMU Wells only BHT - Point

Working Grids.gdb

Columns Within Combo Wells Feature Dataset include 7,843 selectable records that include the following attributes.

Objectid 1
Shape
Objectid
Well Name
APINo
LatDegree
LongDegree
X
Y
Gradient F/ft
Gradient C/M
Gradient C/KM
Gradient Kel/m
Depth Kilometer
BHT C
BHT Kelvin
BHT F
Corrected T
Temperature Unit
Depth of Mea
Depth of M_1
SurfTemp C
SurfTemp F
SurfTemp K

VITA

Adam B. Goodwin was born in Mobile, Alabama and raised in the small city of Satsuma. In May of 2008, Blake graduated from Satsuma High School and one year later joined the United States Navy. In March of 2014, Blake left the Navy and started attending college at the University of South Alabama where he achieved his Bachelor of Science in Geology, May 2017. Throughout his time at South Alabama, Blake worked in the geotechnical industry. He was admitted to the University of Mississippi with a full academic scholarship for the Fall 2017 semester and studied under Dr. Louis Zachos.

Blake's work history includes working in the United States Navy as an aviation structural mechanic, geotechnical engineering at Southern Earth Sciences Inc., and while achieving his masters working as a hydrological engineer at the United States Department of Agriculture. He was also the lead teaching assistant for seven sections of Historical Geology and lead teaching assistant for Geographical Informational Systems (GIS) during the fall of 2017 and spring of 2018. Entering into the fall of 2018 he was awarded a research assistantship through Mississippi Mineral Resources Institute.

Blake's awards and memberships include: The George Lamb Award, 2017 Mobile Rock of Gem Society Award, American Association of Petroleum Geologist, Sigma Gamma Epsilon, and Geology Club of South Alabama.